

**Doctoral Dissertation
(Shinshu University)**

**Cryopreservation and transplantation of rat
pancreatic islets for diabetes therapy model**

March 2021

Takahiro YAMANAKA

Contents

Chapter 1: General introduction	1
Chapter 2: Direct comparison of cryopreservation protocols for rat islets	
Introduction	11
Materials and Methods	12
Results	17
Discussion	21
Abstract	24
Chapter 3: Nylon mesh device for vitrification of large quantities of rat islets	
Introduction	25
Materials and Methods	26
Results	30
Discussion	33
Abstract	35
Chapter 4: Glycemic control by subrenal transplantation of vitrified rat islets	
Introduction	37
Materials and Methods	38
Results	43
Discussion	48
Abstract	50
Chapter 5: Conclusive remark	51
References	55
List of publications	65
Acknowledgements / Funding	67

Abbreviations

Abbreviations used with definition

ANOVA	analysis of variance
AUC	area under the curve
BN	Brown-Norway
COCs	cumulus-oocyte complexes
CPA	cryoprotective agent
DMSO	dimethylsulfoxide
EDT324	EG (30%), DMSO (20%) and trehalose (0.4 M)-based VS
EG	ethylene glycol
ELISA	enzyme-linked immunosorbent assay
FBS	fetal bovine serum
FDA	fluorescein diacetate
GAD	glutamic acid decarboxylase
GSIS	glucose-stimulated insulin secretion
HBSS	Hanks' balanced salt solution
H&E	hematoxylin-eosin
HFV	hollow fiber vitrification
IBMIR	Instant blood-mediated inflammatory reaction
ICA	islet cell antibodies
IEQ	islet equivalent
IPGTT	intraperitoneal glucose tolerance test
IPTR	International Pancreas Transplant Registry
LN ₂	liquid nitrogen
PFA	paraformaldehyde
PI	propidium iodide
qPCR	quantitative PCR
SI	stimulation index
SPF	specific pathogen-free
SSV	solid surface vitrification

STZ	streptozotocin
T1D	type-1 diabetes
T2D	type-2 diabetes
TL	thermolysin-low
VS	vitrification solution
WU	Wünsch Unit

Abbreviations used without definition

cDNA	complementary deoxyribonucleic acid
gDNA	genomic deoxyribonucleic acid
PBS	phosphate-buffered saline
PCR	polymerase chain reaction
RNA	ribonucleic acid
SEM	standard error of the mean
2D / 3D	two dimensional / three dimensional

Abbreviations of genes

<i>Actβ</i>	β-actin
<i>Bax</i>	Bcl-2-associated X protein
<i>Bcl2</i>	B-cell lymphoma 2
<i>Glut2</i>	glucose transporter 2
<i>NeuroD1</i>	neurogenic differentiation 1
<i>Pax6</i>	paired box gene 6
<i>Pdx1</i>	pancreatic and duodenal homeobox 1

Chapter 1 General introduction

Diabetes mellitus is a group of metabolic diseases characterized by hyperglycemia resulting from insulin secretion and/or insulin action defects. The chronic hyperglycemia of diabetes is associated with long-term damage, dysfunction, and failure of different organs, especially the eyes, kidneys, nerves, heart, and blood vessels. Long-term complications of diabetes include retinopathy with the potential loss of vision [1, 2], nephropathy with renal failure [3, 4] and peripheral neuropathy with the risk of foot amputations [5]. Several pathogenic processes, ranging from autoimmune destruction of the pancreatic β -cells with consequent insulin deficiency to abnormalities that result in resistance to insulin action, are involved in the development of diabetes. Deficient insulin action results from inadequate insulin secretion and/or diminished tissue responses to insulin at one or more points in the complex pathways of hormone action. During the last two decades, diabetes patients in the world have increased three times from 151 million (in 2000) to 463 million (in 2019), which suggests one-eleventh of adult people are suffering [6]. It is estimated that 20 million Japanese have diabetes.

The vast majority of diabetes cases fall into two broad etiopathogenetic categories [7], as summarized in **Table 1-1**. Type-1 diabetes (T1D) is caused by a cellular mediated autoimmune destruction of the β -cells of the pancreas and results in an absolute deficiency of insulin secretion. The proportion of T1D patients is estimated to account for only 5–10% of total diabetes patients. However, the incidence of T1D has been increasing worldwide for recent several decades [8], and the studies from Europe and North America expect a two or three folds increase of the T1D children in the coming decades [9]. Individuals at increased risk of developing T1D can be identified by serological evidence of an autoimmune pathologic process occurring in the pancreatic islets and by genetic markers of the immune destruction. The markers include islet cell antibodies (ICA), autoantibodies to insulin, autoantibodies to glutamic acid decarboxylase (GAD) 65, and autoantibodies to the tyrosine phosphatases IA-2 and IA-2 β [10, 11]. Type-2 diabetes (T2D), a much more prevalent category, is caused by a combination of insulin resistance and an inadequate compensatory insulin secretory response (Diabetes Fact sheet Updated November 2017), and accounts for 90–95% of diabetes patients. Individuals with insulin

Table 1-1. Diagnostic criteria for type-1 and type-2 diabetes.

	Type-1 diabetes (T1D)	Type-2 diabetes (T2D)
Manifestation age	Children and young age	Middle or old age
Onset	Acute to subacute	Gradual
Body weight	Thin or normal	Often obese
Insulin secretion	Absent or low	Below normal to high
Insulin resistance	Absent or few	Pronounced
Insulin therapy	Required	Usually not required
Metabolism	Unstable and pronounced	Stable
Autoantibody (GAD, ICA <i>etc.</i>)	90–95% at onset	Absent

Adapted from Kerner *et al.* [7].

resistance and relative (not absolute) insulin deficiency do not need insulin treatment to survive. Other specific types of diabetes are associated with pregnancy and monogenetic defects in β -cell function, which are referred to as gestational diabetes mellitus and maturity-onset diabetes of the young, respectively [12].

The historical background of insulin and diabetes is overviewed in **Table 1-2**. In 1869, German pathological anatomist Langerhans [13] published a doctoral dissertation entitled “Beitrage zur mikroskopischen anatomie der bauchspeicheldrüse (Contributions to microscopic anatomy of the pancreas)” in which pancreatic islets were identified for the first time. Twenty years after the first finding of pancreatic islets, Minkowski & von Mering [14] noticed a swarm of flies feeding on the urine of a pancreas-removed dog and then detected glucose in the urine, suggesting the relationship between the loss of pancreas and the symptom of diabetes. Opie [15] reported some morphological changes in the pancreatic islets of diabetes patients, directly establishing the relationship between the pancreatic islets and diabetes. In 1921, Banting & Best [16] first discovered "insulin" from dog and cattle pancreas, and used it for treatment of diabetes. A British physiologist, Sharpey-Schafer, coined the word "insulin" for the first time as the substance that can be secreted from the pancreas and prevent diabetes [17].

Table 1-2. Research history: Insulin and diabetes.

Years	Events / Findings	Literatures
1869	Discovery of pancreatic islets	Langerhans [13] 
1889	Relationship between pancreas and diabetes	Minkowski & von Mering [14] 
1921	Discovery of insulin	Banting & Best [16] 
1953	Determination of insulin primary structure	Sanger & Thompson [18] 
1966	First surgery of human pancreas transplantation	—
1969	Determination of insulin 3D-structure	Blundell <i>et al.</i> [19] 
2000	Establishment of human islet transplantation	Shapiro <i>et al.</i> [20] 

Novel prize awardees (Insulin-related): F.G. Banting & J.J.R. Macleod (1923), F. Sanger (1958), D.C. Hodgkin (1964), and R.S. Yalow (1977).

Nowadays, it is well known that insulin released from β -cells in the pancreatic islets can control glucose metabolism in the body and its lack leads to increased blood glucose levels and in turn the appearance of glucose in the urine [21]. About 3 million pancreatic islets with 50–500 μm in diameter (1–2% of pancreas volume) are scattered in each human pancreas [22]. A single islet enclosed with fibrous connective tissue capsule contains 20% α -cells producing glucagon, 70% β -cells producing insulin, 5% δ -cells producing somatostatin, and 5% PP-cells producing pancreatic peptide (**Fig. 1-1 A**) [23–25]. Cell composition and structure of the islets are variable among species, as proportionally fewer β -cells and more α -cells in human islets than mouse islets [25, 26]. Rodent islets, unlike the human islets, show the characteristic β -cell core [27]. The primary structure of the insulin was determined by Sanger's group [18, 28], and the three-dimensional structure through X-ray diffraction study by Hodgkin's group [19]. Proinsulin, an 82-amino acid peptide, undergoes folding and formation of 3 disulfide bonds, and is cleaved to yield 51-amino acid active insulin (A-chain: GIVEQCCTSICSLYQLENYCN, B-chain: FVNQHLCGSHLVEALYLVCGERGFFYTPKT) and 31-amino acid C-peptide (**Fig. 1-1 B**) [29]. Paired box gene 6 (*Pax6*), pancreatic and duodenal homeobox 1 (*Pdx1*), *MafA*, and neurogenic differentiation 1 (*NeuroD1*) are responsible genes for insulin transcription [30]. Glucose

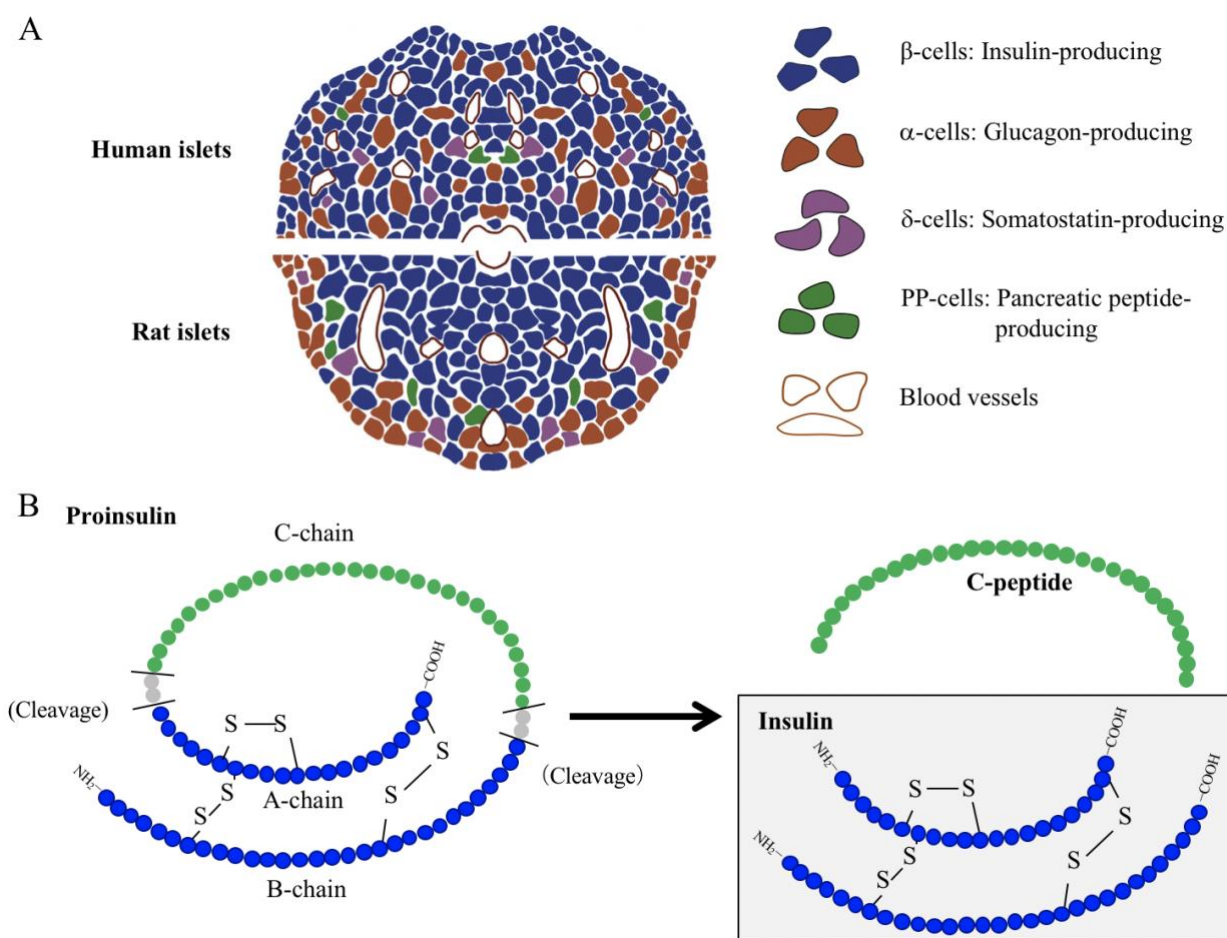


Fig. 1-1. Basic biology of pancreatic islet and insulin. (A) Comparative diagram for human and rat pancreatic islets (modified from Suckale & Solimena [25]). (B) Primary structure of proinsulin / insulin. Each circle shows a single amino acid.

transporter 2 (*Glut2*), constitutively expressing in β -cells, acts as a glucose sensor and regulates insulin secretion. A master gene of β -cell and pancreas, *Pdx-1*, is an upstream regulator of the *Glut2* [31–33].

Diabetes therapy

Insulin therapy decreases the aggravation rate of diabetic complications, but increases the risk of hypoglycemia [34]. The β -cell replacement therapy, performed as transplantation of whole pancreas or pancreatic islets, can benefit the therapeutic option to restore normoglycemia in patients suffering T1D and, at least in part, T2D. Pancreas transplantation, first performed in 1966, was originally plagued by a high rate of technical failures until both surgical technique and

immunosuppression were established. According to the International Pancreas Transplant Registry (IPTR), mean successful pancreas transplantation rates with 1-year insulin independence were 77% (simultaneous pancreas-kidney transplantation), 53% (pancreas transplantation following kidney transplantation) and 52% (pancreas transplantation alone) in the years of 1987–1993 [35]. These rates were improved to 86% (simultaneous pancreas-kidney transplantation), 80% (pancreas transplantation following kidney transplantation) and 78% (pancreas transplantation alone) in the years of 2006–2010. Recent 5-year graft function rates by IPTR were 72, 55, and 55% for simultaneous pancreas-kidney transplantation, pancreas transplantation following kidney transplantation, and pancreas transplantation alone, respectively [36].

Islet transplantation is considered as a useful option for the clinical treatment of T1D patients since the Edmonton protocol has been established in 2000 [20]. The 1-year insulin independence was achieved at 80% in 65 patients transplanted with islets, but long-term follow-up of this initial Edmonton cohort showed that only 10–15% remained off-insulin at five years [37]. However, it was noted that many patients who returned to insulin dependence exhibited a reduced insulin requirement and a less frequent occurrence of hypoglycemia, indicating the persistence of meaningful β -cell survival [38]. Thus, a long-term glycemic control without frequent injections of insulin can be attained by the islet transplantation with an improved protocol, but the islet yield isolated from single donors is not high enough for the transplantation, requiring the participation of multiple donor pancreases to increase islet availability [39, 40]. Given the wide distribution of islet size, individual islets are converted to the islet equivalent (IEQ; islet of a diameter of 150 μm is defined as 1 IEQ) [41]. A huge number of islets (10,000–12,000 IEQ/kg recipient body weight) is required for clinical transplantation [20, 42], because the considerable loss of transplanted islets occurs due to instant blood-mediated inflammatory reaction (IBMIR) [43, 44] and exposure to hypoxia and low nutrient availability until vascularization.

Intrahepatic transplantation by portal vein infusion of islets is the most common clinical approach to cure T1D patients. Several alternative deposition sites by islet transplantation have been investigated in experimental animal models (**Fig. 1-2**), which include the pancreas, thymus, spleen, bone marrow, cerebral ventricles, anterior eye chamber, kidney subcapsule, intra-muscle,

intraperitoneal or subcutaneous space, omental pouch, and gastrointestinal wall [45–47]. An optimal transplantation site should be readily accessible, bear an adequate tissue volume, have a sufficient vascular network, and support the islets to prevent loss of function and cell death. Furthermore, the ability to retrieve and monitor the islet engraft may be desirable for transplantation sites. In rodent models, subrenal transplantation by islet deposition beneath kidney capsule is often used due to reproducibility and relatively small islet number required per recipient [47].

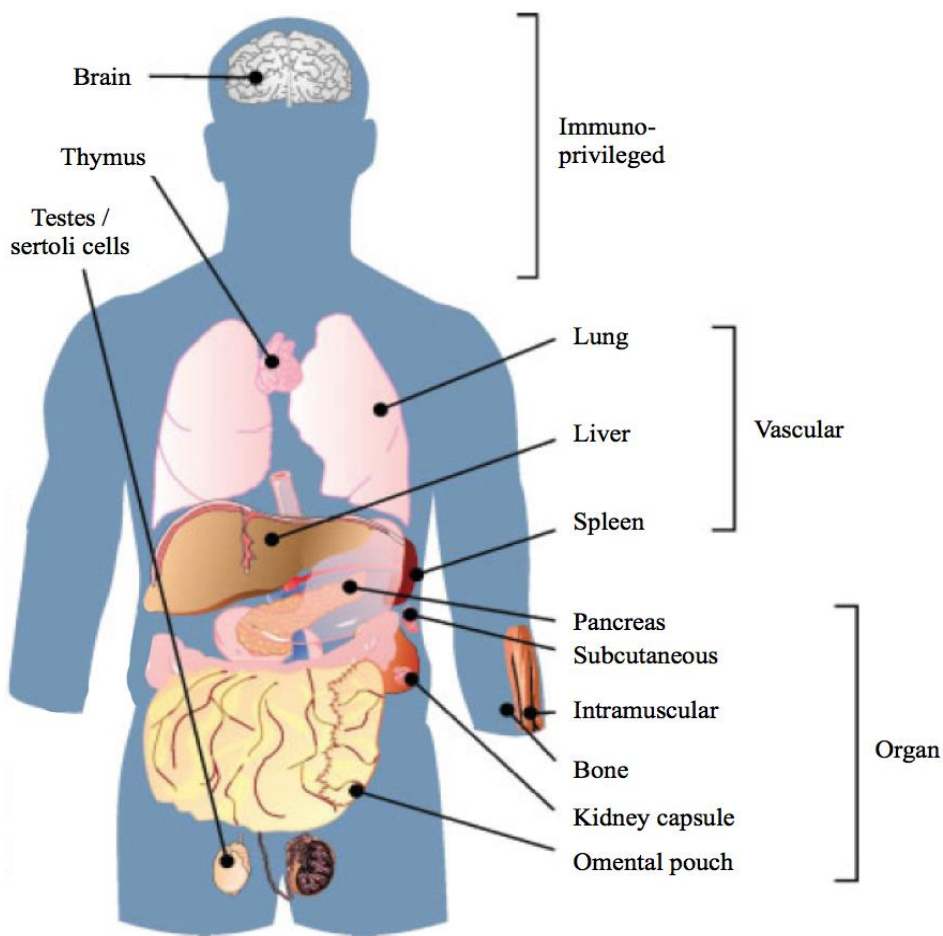


Fig. 1-2. Experimental and clinical islet transplantation sites (modified from Marani *et al.* [47]).

Islet cryopreservation

Cryopreservation of pancreatic islets without functional loss can overcome the inevitable shortage of donors and allow time to investigate immunological tissue matching between donors and recipients. Islet cryopreservation in liquid nitrogen (LN₂) was initiated with a conventional

cell freezing protocol in rats [48] and humans [49, 50], with poor post-thaw survival rates of approximately 50% [51]. It is an advantage of freezing protocol that a large amount of cell populations can be stored without special skills. Neutral low molecular weight amphiphilic solute, such as dimethylsulfoxide (DMSO) or ethylene glycol (EG), has been used as a permeable cryoprotective agent (CPA), to reduce the amount of intracellular ice crystals (**Fig. 1-3 A**). During slow cooling (0.3–1.0°C/min) from relatively high subzero temperature to –80°C, cells are fully dehydrated to extracellular unfrozen CPA-concentrates, and then can be stabilized after rapid cooling to –196°C (**Fig. 1-4 A**). The slow cooling process can be terminated at approximately –30°C, to make cells moderate-dehydrated (time-savable "two-step freezing" regimen). The optimal thawing rate is determined by the volume of intracellular ice crystals and amorphous glass existing at –196°C. Fully dehydrated cells with little ice/glass must be thawed at a slower rate (4–25°C/min) to minimize osmotic damages by a rapid influx of water into cells during thawing, while partially dehydrated cells with a certain volume of ice/glass are thawed rapidly (> 2,000°C/min) not to suffer physical damages by re-crystallization. However, detrimental ice crystal formation cannot be avoided in any freezing protocols, which may disrupt islet capsule and impair insulin secretion [52, 53]. This dysfunction in post-thaw islets results in the requirement of transplanting more than double the IEQ, compared with fresh islets, to achieve normoglycemia [41, 52]. Since the islets are composed of several different cell types with paracrine intercellular communications, they may be sensitive to cryoinjuries induced by ice crystals.

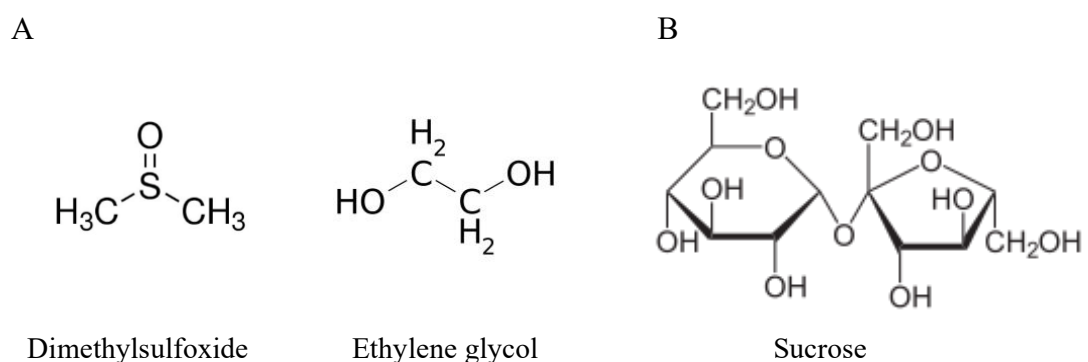


Fig. 1-3. Structure of typical chemicals used as (A) membrane permeable CPA and (B) membrane non-permeable CPA.

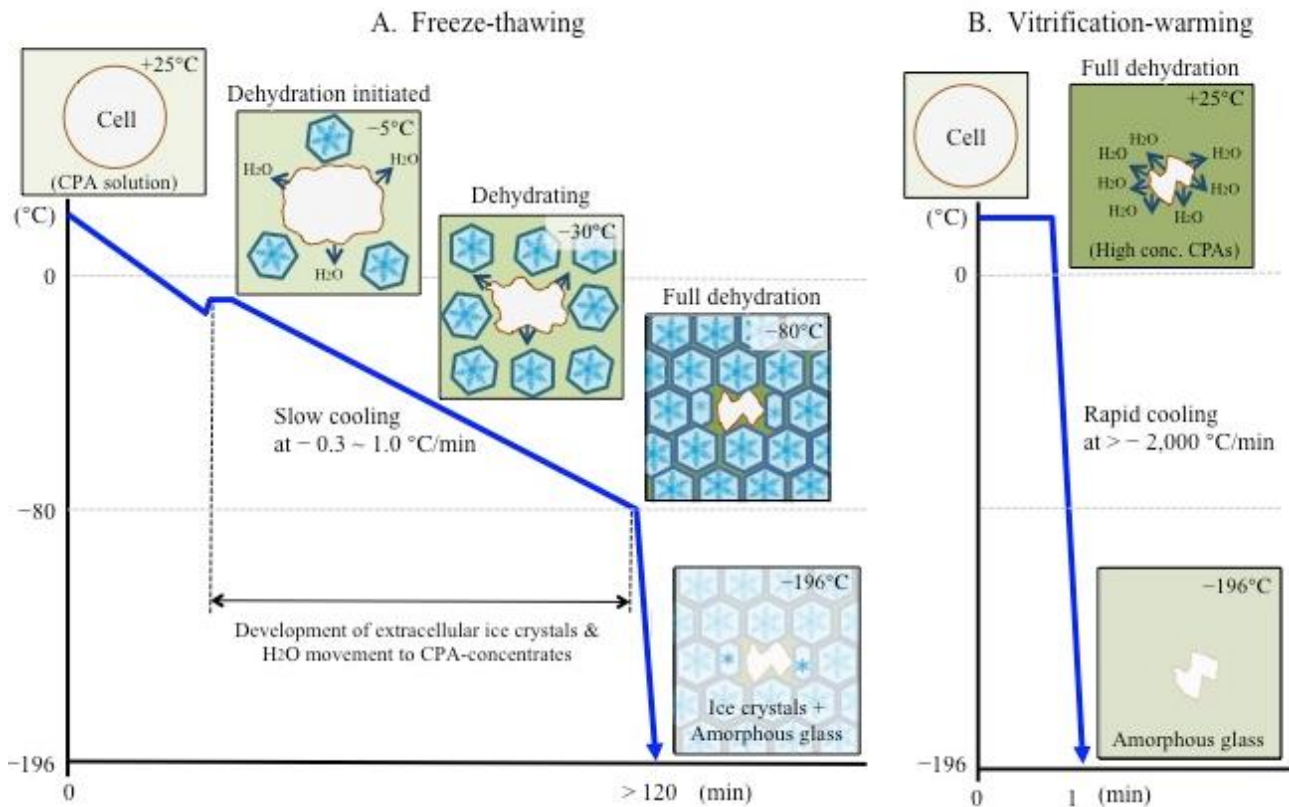


Fig. 1-4. Cryoprotective theory: The interactions among CPAs, temperature and cell dehydration. (A) Freeze-thawing: Cells are dehydrated by concentrating extracellular CPAs during slow cooling process at relatively high subzero temperatures. (B) Vitrification-warming: Vitrification solution contains highly concentrated CPAs capable of cell dehydration at an ambient temperature instead, and contributes to the formation of innocent ice (amorphous glass) during rapid cooling procedure.

To avoid the ice crystal formation, a vitrification protocol has been developed with highly concentrated CPA solution and applied to various cell types, including preimplantation embryos [54, 55]. Cells are fully dehydrated in an osmotic response to vitrification solution containing highly concentrated membrane permeable CPAs (*e.g.*, DMSO and/or EG) plus non-permeable CPAs (*e.g.*, sucrose; **Fig. 1-3 B**), before direct plunging into LN₂ (**Fig. 1-4 B**). Although attempts at cryopreserving the islets by vitrification resulted in a recovery of functional islets [56, 57], a considerable loss in post-warm islet viability and insulin secretion has been reported [58, 59]. Improved vitrification protocols, characterized by ultra-rapid cooling procedure, made banking of unfertilized oocytes more practical in human infertility clinics [60]. As the disadvantageous

aspects, such an improved vitrification protocol requires unique cryodevices (*e.g.*, microgrid [61], open-pulled straw [62], Cryoloop [63], Cryotop [64]) and complicated stepwise CPA treatments, and limits the sample number that can be loaded on the cryodevices (recommended quantity 10–12, possible upper limit 20–30 per cryodevice). Matsumoto *et al.* [65] reported that as many as 65 bovine immature cumulus-oocyte complexes (COCs) could be vitrified-warmed using nylon mesh as cryodevice, with subsequent work by Abe *et al.* [66] successfully producing a calf from these vitrified-warmed COCs.

The present study was designed to establish a novel cryopreservation protocol for a higher yield of functional pancreatic islets in the rat diabetes therapy model. The thesis is composed of three independent experimental series. In the first series of experiments, cryosurvival, insulin secretion potential, and expression of β -cell function-associated genes in inbred rat islets were directly compared between conventional Bicell[®] freezing and Cryotop[®] vitrification protocols. Islet size-dependent sensitivity to Cryotop[®] vitrification was also investigated (Chapter 2). In the second series of experiments, a nylon mesh device processed as a developed figure of a triangular pyramid was used for vitrification of a large quantity of rat islets (up to 100), to overcome a technical limit of Cryotop[®] vitrification in sample number loadable per device. Two *in vitro* parameters, such as cryosurvival and insulin secretion potential, were investigated (Chapter 3). In the last series of experiments, syngeneic subrenal transplantation was conducted to confirm the adaptability of rat islets vitrified-warmed on the nylon mesh device (100 islets per device) to glycemic control in diabetic model rats. The *in vivo* assay included monitoring blood glucose levels and the glucose tolerance test of cured recipients. Angiogenesis in the islet engrafts was evaluated histologically (Chapter 4).

Chapter 2 Direct comparison of cryopreservation protocols for rat islets

2.1. Introduction

Successful cryopreservation of highly functional islets for an indefinite period would allow islet transplantations in remote areas. Islet cryopreservation was initiated with a conventional cell freezing protocol in rats [48] and humans [49, 50], with poor post-thaw survival rates of approximately 50% [51]. The freezing protocol has an advantage as a large amount of cell populations can be stored without special skills. However, detrimental ice crystal formation cannot be avoided in any freezing protocols, which may disrupt islet capsule and impair insulin secretion [52, 53]. This dysfunction in post-thaw islets results in the requirement of transplanting more than double amounts of post-thaw islets, compared with fresh islets, to achieve normoglycemia [41, 52]. Since the islets are composed of several different cell types with paracrine intercellular communications, they may be sensitive to cryoinjuries induced by ice crystals.

Cells exposed to highly concentrated CPA solution can be fully dehydrated and transformed into an amorphous state during the subsequent rapid cooling process. This method is referred to as vitrification and applied to various cell types [54, 55]. The attempts to preserve the islets by vitrification resulted in a recovery of functional islets [56, 57]. However, a considerable loss in post-warm islet viability and insulin secretion was reported [58, 59]. Further improvement of vitrification protocols as an ultra-rapid cooling procedure made banking of unfertilized oocytes more practical in human infertility clinics [60]. As the disadvantage aspects, such an improved vitrification protocol requires unique cryodevices (*e.g.*, microgrid [61], open-pulled straw [62], Cryoloop [63], Cryotop [64]) and complicated stepwise CPA treatments. The conventional vitrification protocol limits the sample number that can be loaded on the cryodevices (recommended quantity 10–12, possible upper limit 20–30 per cryodevice).

The aim of the present study was to determine the optimal cryopreservation protocol for rat pancreatic islets. In the first study, cryosurvival, gene expression and glucose-stimulated insulin secretion (GSIS) were directly compared between conventional Bicell[®] freezing and Cryotop[®] vitrification. Islet size-dependent sensitivity to Cryotop[®] vitrification was also investigated.

2.2. Materials and Methods

Experimental design

Cryosurvival of isolated rat pancreatic islets (size category: 101–150 μm in mean longest and widest diameter) following Bicell[®] freezing protocol and Cryotop[®] vitrification protocol was assessed by fluorescein diacetate (FDA) / propidium iodide (PI) double staining. Expression of genes relating to β -cell function (*Pdx1* and *Glut2*) and one of the apoptotic pathways (*Bax* and *Bcl2*) was assessed by quantitative PCR (qPCR). The stimulation index (SI) in GSIS was measured with an enzyme-linked immunosorbent assay (ELISA) kit. In an additional experiment, the survival and SI of vitrified-warmed islets with different size category (101–150, 151–200, 201–250, 251–300 and 301–350 μm) were investigated immediately after warming.

Chemicals and animals

Unless otherwise indicated, chemicals used in this study were purchased from Sigma-Aldrich Corp. (St. Louis, MO, USA). The specific pathogen-free (SPF) Brown-Norway (BN) rats were purchased from Japan SLC, Inc. (Shizuoka, Japan). The rats were housed in an environmentally controlled room with a 12-h dark / 12-h light cycle at a temperature of $23 \pm 3^\circ\text{C}$, with free access to a laboratory diet (NMF; Oriental Yeast Co., Ltd., Tokyo, Japan) and tap water. All animal experiment procedures were reviewed and approved by the Animal Care and Use Committee of the Shinshu University, Nagano, Japan. Animals were treated humanely and the standards conformed to those of current ethical animal research practices.

Isolation of rat islets

Pancreatic islets were isolated from male rats at 8–12 weeks old. Briefly, the bile duct of the rats was cannulated with a fine plastic tube (**Fig. 2-1 A**) and the pancreas was distended with approximately 8 mL of liberase thermolysin-low (TL) solution (1 Wünsch Unit [WU]/mL liberase in cold Hanks' balanced salt solution [HBSS]) (**Fig. 2-1 B**). The pancreas was excised, minced, and incubated at 37°C for 30 min, and then the digested tissues were purified on a discontinuous histopaque gradient that was layered with histopaque1119, histopaque1077, and 2% fetal bovine serum (FBS; HyClone[™], GE Healthcare Life Science, Logan, UT, USA) in HBSS. Islets were

handpicked using capillary pipettes (inner diameter: 150, 200, 250, 300 or 350- μm) under a stereomicroscope (**Fig. 2-1 C**), and cultured for 24 h in 2 mL of RPMI-1640 (Product No. 11835-030; Life Technologies Inc., Rockville, MD, USA) supplemented with 10% FBS and antibiotics (100 units/mL penicillin and 100 $\mu\text{g/mL}$ streptomycin) at 37°C in a humidified atmosphere of 5% CO₂ in air until use for cryopreservation. This commercially available RPMI-1640 medium contained glucose at a concentration of 11 mM.

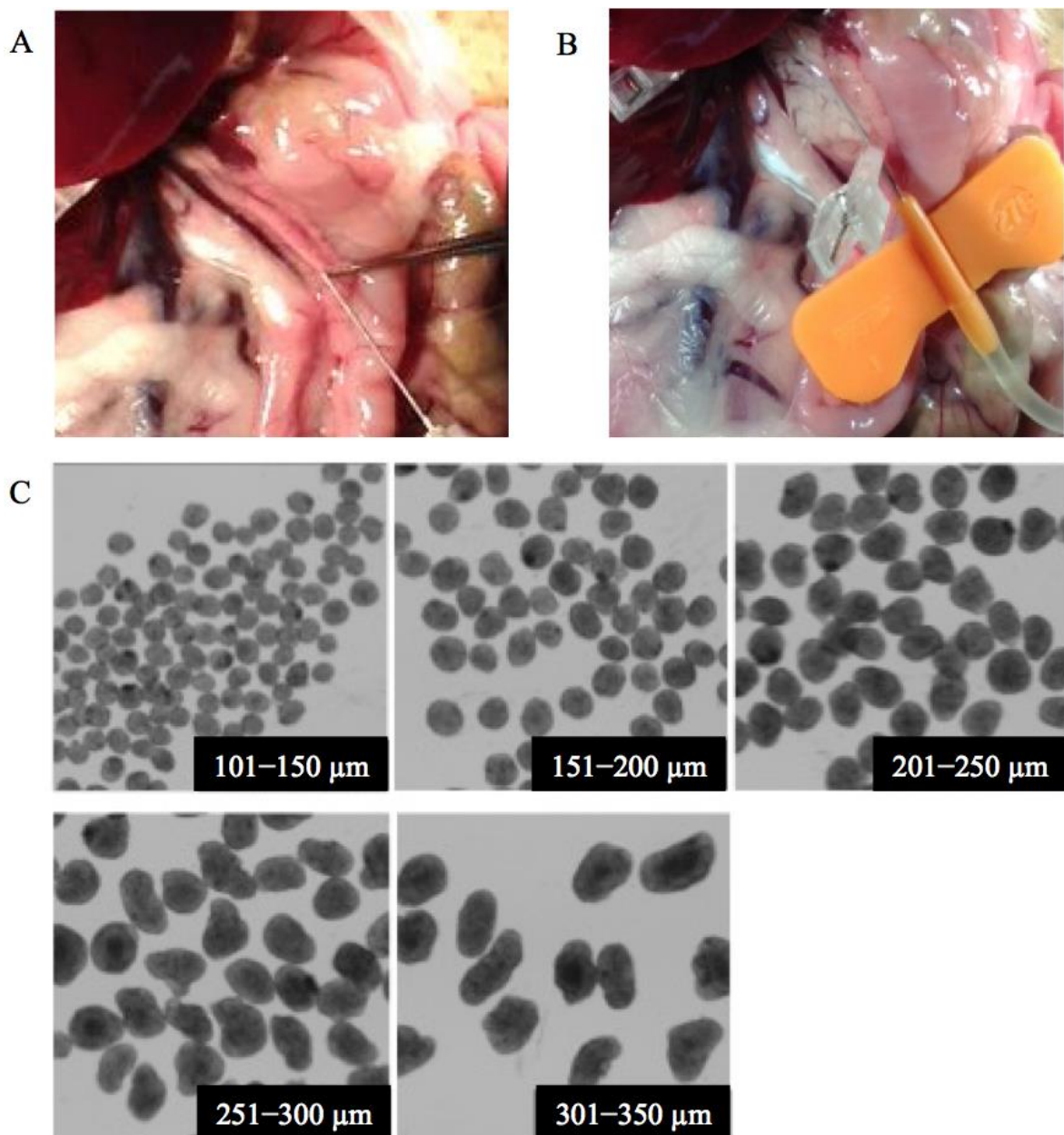


Fig. 2-1. Isolation of rat pancreatic islets. (A) Cannulation of bile duct. (B) Perfusion of pancreas with liberase TL solution. (C) Isolated pancreatic islets with different size category.

Cryopreservation

According to the manufacturer's instruction manual, a conventional freezing protocol was conducted using Bicell[®] bio freezing vessels (Nihon Freezer Co., Ltd., Tokyo, Japan). Briefly, islets were exposed to 15% DMSO in RPMI-1640 containing 10% FBS and antibiotics for 15 min at ambient temperature, and then cooled to 4°C for 15 min. Fifty islets were placed in a precooled cryotube containing 500 µL of the above-mentioned CPA solution, and the cryotubes were packed into a Bicell[®] vessel (**Fig. 2-2 A**). Subsequently, the Bicell[®] vessel was placed in a -80°C deep freezer overnight (estimated cooling rate, -0.5°C/min during the first 3 h), and then the cryotubes were transferred into LN₂. After storage for at least 1 week, the cryopreserved islets were thawed by gently warming the cryotubes in a 37°C water bath for 1 min. Following thawing, islets were transferred to RPMI-1640 containing 10% FBS, antibiotics, and sucrose in a stepwise manner (1.0, 0.5, 0.25, and 0 M sucrose for 2, 3, 5, and 5 min, respectively).

Cryotop[®] vitrification was conducted as described previously [67]. Briefly, islets were equilibrated with 7.5% EG (Wako Pure Chemical Industries, Ltd., Osaka, Japan) and 7.5% DMSO (Wako) in RPMI-1640 supplemented with 20% FBS for 3 min at ambient temperature (25 ± 2°C), and then transferred into a vitrification solution (VS) comprising 15% EG, 15% DMSO, and 0.5 M sucrose as CPAs in RPMI-1640 containing 20% FBS for 60 sec at ambient temperature. Within this 60-sec period, 10 islets were loaded onto the 0.1 × 0.7 × 20 mm polypropylene strip of a Cryotop[®] device (**Fig. 2-2 B**) (Kitazato Corp., Shizuoka, Japan) with a minimal volume of the VS, and then quickly plunged into LN₂. After storage for at least 1 week, islet warming was performed by immersing the polypropylene strip of Cryotop[®] into RPMI-1640 containing 20% FBS and 1 M sucrose at 38.5°C for 1 min. Following warming, islets were transferred to RPMI-1640 containing 20% FBS and sucrose in a stepwise manner (0.5, 0.25, and 0 M sucrose for 3, 5, and 5 min, respectively).

Survival assay

Islet survival was assessed by double staining with membrane exclusion dyes, FDA and PI. An aliquot of 10 islets in each group was stained with 25 µg/mL FDA and 25 µg/mL PI for 30 sec in a dark condition. After being washed three times in PBS, the FDA (green) / PI (red)

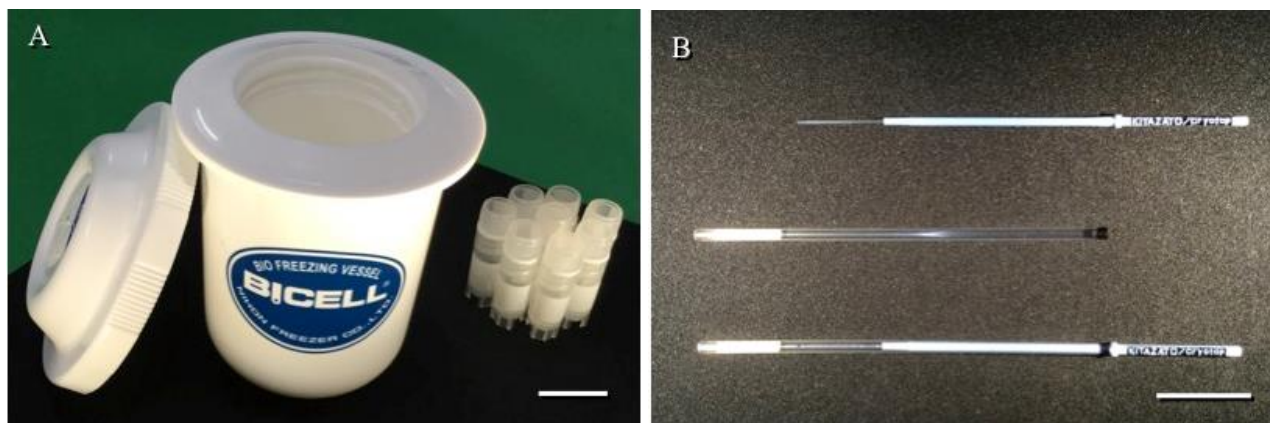


Fig. 2-2. Photographs of Bicell® freezing vessel with 8 cryotubes (A) and Cryotop® vitrification device with covering straw (B). Scale bars = 2-cm.

fluorescent images were taken by an epifluorescence microscope (IX73; Olympus Corp., Tokyo, Japan). The fluorescent area was quantified using Image J software (<https://imagej.nih.gov/ij/>). The baseline cutoff of fluorescent signals was performed by using the automatic data processing function of the Image J software. The survival rate was calculated as: $100 \times \text{FDA-positive area} / (\text{FDA-positive area} + \text{PI-positive area})$. To identify the localization of the PI-positive dead cells, islets were fixed in 4% paraformaldehyde (PFA) for 30 min and stained with FDA and PI, as described above. Preparations were mounted with coverslips in an antifade agent (100 mg 1,4-diazabicyclo [2.2.2] octane in 1 mL glycerol), and images were taken at the largest section of the islets, using a confocal laser microscope (FV1000-D; Olympus).

Quantitative PCR

Total RNA was extracted from islets using the Sepasol®-RNA I Super G kit (Nacalai Tesque Inc., Kyoto, Japan), and the first-strand cDNA was synthesized using the ReverTra Ace qPCR RT Master Mix with gDNA Remover (Toyobo Co., Ltd., Osaka, Japan). Primers for *Pdx1* (pancreatic and duodenal homeobox 1), *Glut2* (glucose transporter 2) *Bax* (Bcl-2-associated X protein), *Bcl2* (B-cell lymphoma 2) and *Actβ* (β-actin) in qPCR were listed in **Table 2-1**. The qPCR was performed to detect fold changes of *Pdx1*, *Glut2* (β-cell function regulatory genes), *Bax*, *Bcl2* (apoptosis pathway-relating genes) and *Actβ* (internal reference gene) expression using a Thermal Cycler Dice Real Time System (TaKaRa Bio Inc., Shiga, Japan) and the SYBR® *Premix Ex Taq*™ II reagent. Values were normalized to *Actβ*.

Table 2-1. Primer sequences used for quantitative real-time PCR.

Gene	Forward primer (5'-3')	Reverse primer (5'-3')
<i>Pdx1</i>	TGGATGAAATCCACCAAAGC	TGTAGGCTGTACGGGTCCTC
<i>Glut2</i>	GCTGGAAGAAGCGTATCAGG	AATCCTGATTGCCCAGAATG
<i>Bax</i>	CTGCAGAGGATGATTGCTGA	GATCAGCTCGGGCACTTTAG
<i>Bcl2</i>	CGACTTTGCAGAGATGTCCA	ATGCCGGTTCAGGTACTCAG
<i>Actβ</i>	ATTGCTGACAGGATGCAGAA	TAGAGCCACCAATCCACACAG

Insulin secretion

The functionality of cryopreserved or fresh islets was assessed by static GSIS assay [68]. Briefly, islets (10 each per group; immediately after thawing/warming or after 24 h culture) were washed three times with RPMI-1640 / 10% FBS containing 3 mM glucose and preincubated 1 h at 37°C in a humidified atmosphere of 5% CO₂ in air. Then, the islets were stimulated by transferring into the RPMI-1640 / 10% FBS containing 20 mM glucose and incubated for 1 h as described above. At the end of preincubation and incubation, supernatants were collected and stored at -80°C until the insulin assay. The basal and stimulated insulin levels (ng/islet/h) were determined by an ELISA kit for rat insulin (MioBS Inc., Kanagawa, Japan), and the SI was defined to be: the stimulated insulin level in response to 20 mM glucose divided by the basal level in response to 3 mM glucose.

Statistical analysis

Percentage data were subjected to arcsine transformation before statistical analysis. Differences between groups were assessed by one-way analysis of variance (ANOVA). When ANOVA was significant, differences among values were analyzed by Tukey's Honest Significant Difference test or Dunnett's test for multiple comparisons. Data were considered statistically significant at $P < 0.05$.

2.3. Results

Cryosurvival

The difference in survival rates of rat islets immediately after cryopreservation was not significant (50 and 57% in Bicell[®] freezing and Cryotop[®] vitrification, respectively), as shown in **Fig. 2-3 A**. On the other hand, these cryosurvival rates were lower than the survival rate of fresh control islets (90%). When the vitrified-warmed islets were cultured for 24 h, the survival rate (85%) approached to that of fresh control islets (91%), as shown in **Fig. 2-3 B**. However, the recovery culture of frozen-thawed islets did not increase the survival rate (58%). In order to identify the target area of cryoinjury, confocal FDA / PI images of cryopreserved islets were analyzed. Most of the PI-positive dead cells in post-warm islets were detected on their peripheral area, while the dead cells in post-thaw islets distributed not only in their peripheral area but also in the center (**Fig. 2-3 C**, upper panels). Epifluorescent FDA and PI images corresponding to the mean values of 3 experimental groups in **Fig. 2-3 A** were shown in the middle and bottom panels of **Fig. 2-3 C**. Vitrified-warmed islets after 24 h culture appeared to be morphologically normal (**Fig. 2-3 D**).

Gene expression

Bicell[®] freezing tended to affect the *Pdx1* expression ($P = 0.051$) and significantly affected the *Glut2* expression ($P < 0.05$), as shown in **Fig. 2-4**. The expression of these genes was not different between islets before and after Cryotop[®] vitrification. On the other hand, there were no significant changes in the expression of genes relating to the apoptotic pathway (*Bax*, *Bcl2*, and *Bax / Bcl2* ratio) of cryopreserved islets as well as fresh control islets. The ratio of *Bax* to *Bcl2* shows relative resistance to stimuli capable of triggering cell death.

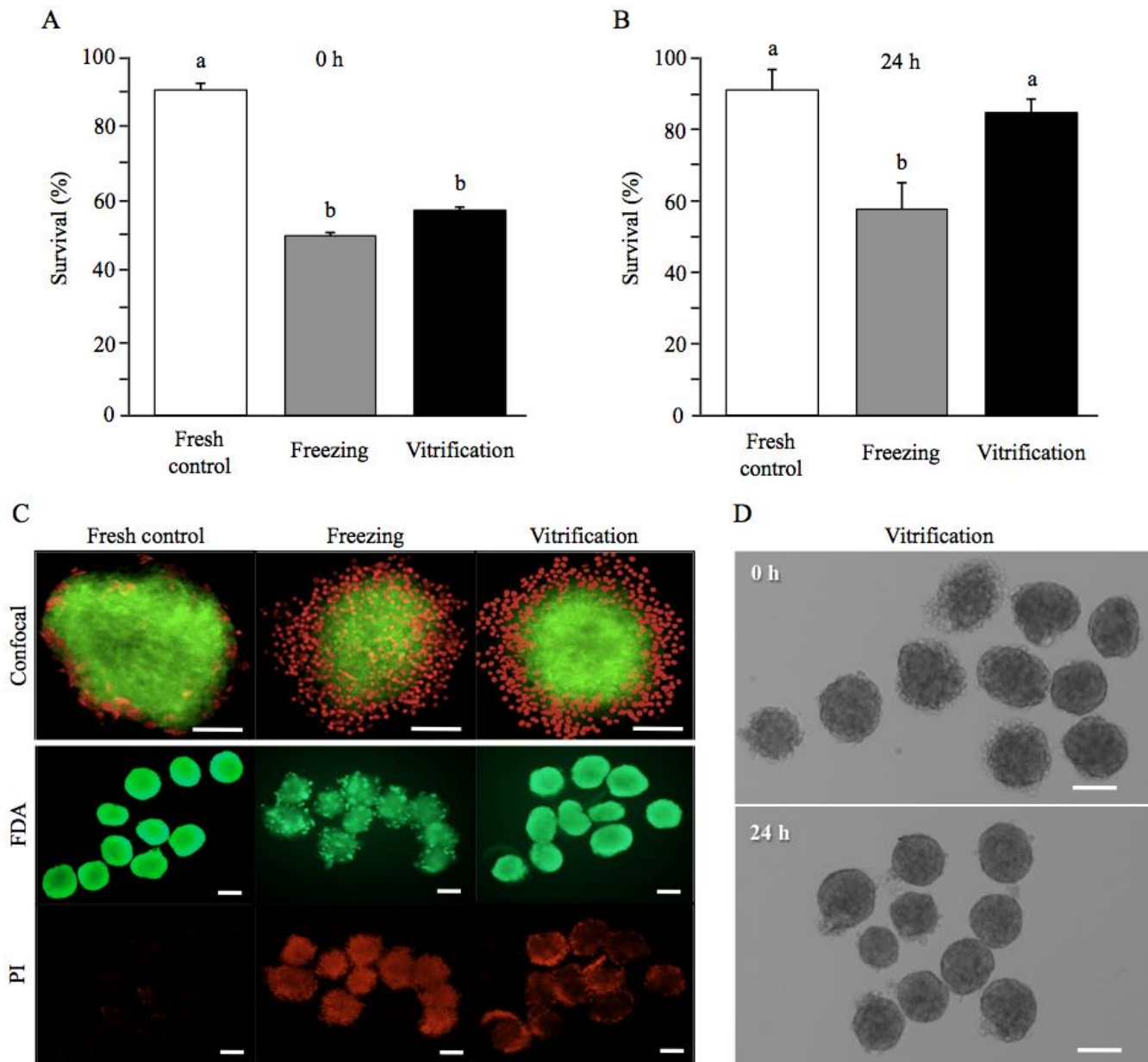


Fig. 2-3. Cryosurvival of rat islets after Bicell[®] freezing and Cryotop[®] vitrification. (A) Survival immediately after thawing/warming. (B) Survival after 24 h recovery culture. Data are expressed as the mean \pm SEM of 5 replicates (0 h) or 3 replicates (24 h) in each group. Different letters represent significantly different groups ($P < 0.05$). (C) Islets stained with FDA and PI. Upper: merge of confocal images, Middle and bottom: epifluorescent images, which are the representative images showing the mean values of 3 experimental groups in the above panel-A. The survival rates in fresh control, Bicell[®] freezing and Cryotop[®] vitrification groups were estimated as 90, 50 and 57%, respectively. (D) Islet morphology after vitrification and warming. Upper: Islets immediately after warming (0 h), Bottom: Islets after culture (24 h). Scale bars = 100- μ m.

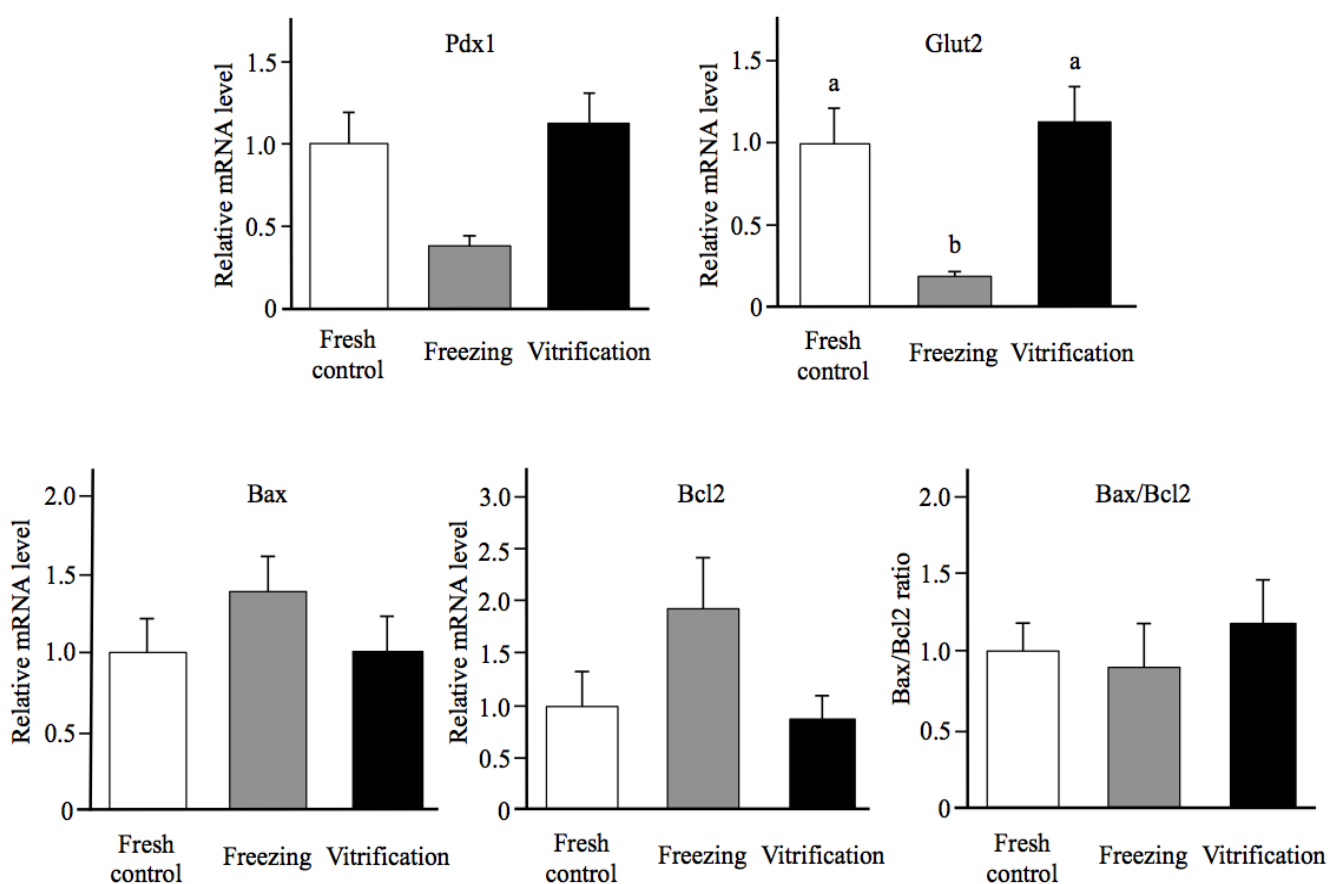


Fig. 2-4. Gene expressions in rat islets after cryopreservation. Data are expressed as the mean \pm SEM of at least 4 replicates in each group. Different letters represent significantly different groups ($P < 0.05$).

Insulin secretion

The basal level of insulin secretion in response to the low concentration of glucose was higher in frozen-thawed islets than fresh control or vitrified-warmed islets (**Table 2-2**). However, the stimulated insulin secretion level in response to the high concentration of glucose was comparable among fresh control, Bicell[®] freezing and Cryotop[®] vitrification groups. Therefore, the SI significantly differed between fresh control and Bicell[®] freezing groups (6.7 and 1.9, respectively) and the SI in Cryotop[®] vitrification group (3.9) was the intermediate. A similar likelihood of insulin secretion was observed when the post-thaw / post-warm islets were cultured for 24 h.

Table 2-2. GSIS assay from frozen *versus* vitrified rat islets.

Culture period (h)	Group	3 mM glucose (ng/islet/h)	20 mM glucose (ng/islet/h)	Stimulation index
0	Fresh control	0.12 ± 0.03 ^a	0.85 ± 0.29	6.7 ± 0.9 ^a
	Freezing	0.74 ± 0.06 ^b	1.44 ± 0.43	1.9 ± 0.5 ^b
	Vitrification	0.27 ± 0.07 ^a	1.03 ± 0.36	3.9 ± 1.0 ^{ab}
24	Fresh control	0.09 ± 0.03 ^a	0.33 ± 0.09 ^a	4.1 ± 0.7 ^a
	Freezing	0.50 ± 0.12 ^b	0.93 ± 0.15 ^b	1.9 ± 0.1 ^b
	Vitrification	0.19 ± 0.09 ^a	0.40 ± 0.13 ^a	3.1 ± 0.5 ^{ab}

Data are expressed as the mean ± SEM of at least 4 replicates in each group.

^{a,b} Different superscripts represent significantly different groups ($P < 0.05$).

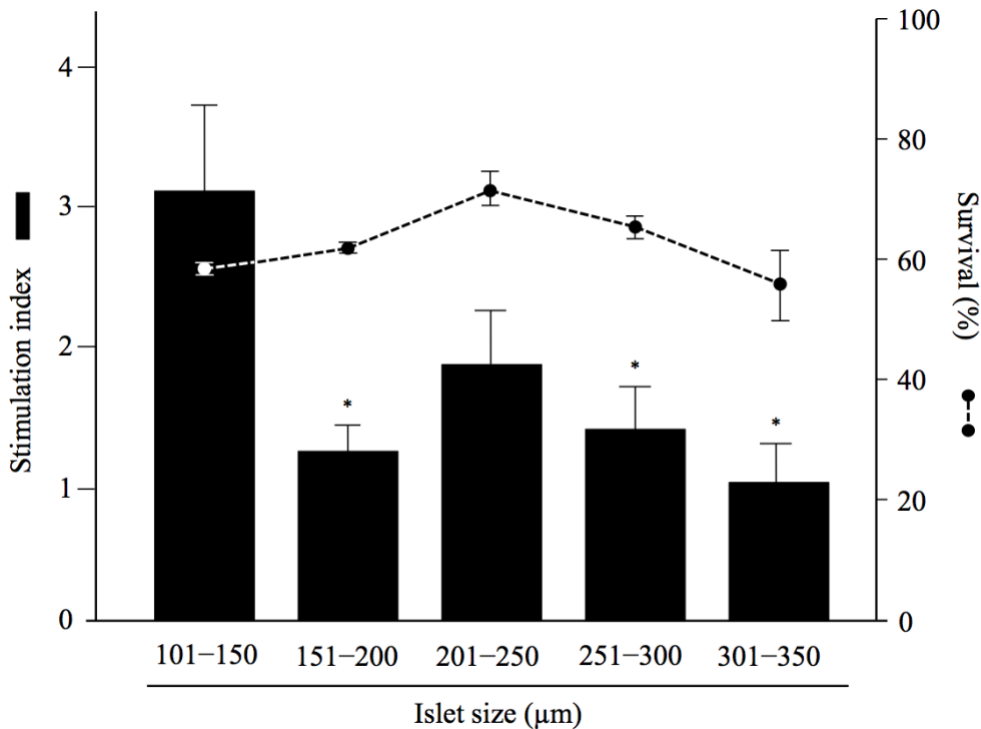


Fig. 2-5. Effect of larger islet size on the survival and insulin secretion after Cryotop[®] vitrification. Closed circles with dot line: Cryosurvival, Columns: Stimulation index (SI). Data are expressed as the mean ± SEM of 3 replicates (cryosurvival) or 4 replicates (SI) in each group. Asterisks represent significant differences from the control 101–150 µm size category group ($P < 0.05$).

Islet size effect

It was investigated whether Cryotop[®] vitrification protocol is applicable to the larger size islets without any modifications in the CPA pretreatment or exposure time to vitrification solution. When the islet harvests were classified into 5 groups (101–150, 151–200, 201–250, 251–300 and 301–350 μm in mean diameter), the FDA / PI staining of post-warm islets showed no significant difference in their cryosurvival rates (**Fig. 2-5**). However, function of the post-warm islets, assessed by insulin secretion, was impaired as the islet size increased.

2.4. Discussion

Two cryopreservation protocols, in which vessels (Bicell[®]) / devices (Cryotop[®]) are commercially available, were compared for their potential to recover the functional rat pancreatic islets (Experiment 1). Bicell[®] freezing can provide a constant slow cooling rate ($-0.5^{\circ}\text{C}/\text{min}$) in -80°C deep freezer and widespread mainly for non-cultured or cultured single animal cells, including various cell lines, pluripotent embryonic stem cells and feeder cells. Cryotop[®] vitrification has been developed to accelerate cooling rate ($-23,000^{\circ}\text{C}/\text{min}$) when the devices are plunged into LN_2 , and applied mainly for cryopreservation of the larger ($> 100 \mu\text{m}$ in diameter) mammalian embryos and oocytes. We are well-acquainted with both protocols [67, 69, 70]; the difference in skill maturity often causes controversial results among cryopreservation protocols. Considering the glycemic control by islet transplantation, the higher islet recovery rate is desired not only in survival but also in insulin secretion [53, 71, 72]. As rat islets were dysfunctional after conventional freezing and thawing, more than double post-thaw islets were required to restore normoglycemia by their transplantation compared to the non-frozen fresh islets [49, 52]. Islet insulin secretion potential measured in vitro is closely related to the in vivo response for glycemic control [49, 68]. Using this in vitro parameter (SI), Sasamoto *et al.* [68] suggested the higher suitability of vitrification than conventional slow freezing in rat islets, whereas Agudelo and Iwata [73] reported a comparable result between vitrification and freezing in hamster islets.

In the present study, islet cryosurvival was determined by area-based calculation from FDA / PI double stained samples (**Fig. 2-3**), resulting in a comparable incidence of cryoinjury between

Bicell[®] freezing and Cryotop[®] vitrification. Corominola *et al.* [49] reported that survival rates of fresh and frozen-thawed rat islets were 98 and 82% respectively. They also observed a higher cryosurvival rate after 24 h post-thaw culture (93%), with little increase in the SI value from 1.7 to 2.0. Since most of the PI-positive dead cells were detected in the peripheral area of vitrified-warmed islets (**Fig. 2-3 C**), their liberation during the subsequent 24 h culture would lead to an increased survival rate (**Fig. 2-3 B, D**). Evenly distributed dead cells in frozen-thawed islets may be due to the formation of detrimental ice crystals. Supplementation of synthetic antifreeze glycoprotein to DMSO solution inhibited cryoinjuries of rat islets by preventing ice crystal formation [74]. Using a histological approach, Sakonju *et al.* [75] observed clusters of necrotic cells at the center of rat islets cryopreserved by two-step freezing. It should be noted that Bicell[®] freezing protocol does not include any ice-seeding treatments which can be applied in two-step freezing regimens using a programmable freezer. *Bax* triggers the release of mitochondrial apoptogenic factors such as cytochrome *c*, whereas *Bcl2* inhibits this release. Therefore, the *Bax* / *Bcl2* ratio is a critical determinant of relative resistance to detrimental stimuli [50]. Analysis by qPCR indicated that *Bax* / *Bcl2* ratio was not affected by the cryopreservation protocols employed (**Fig. 2-4**), suggesting that cell death in cryopreserved islets is caused by necrosis. Little information is available for the apoptotic pathway-relating gene expression in cryopreserved islets. Liu *et al.* [76] reported that a similar level of Bax protein was detected in rat islets preserved for 24 h at 37°C and –80°C, but the level of Bcl2 protein was not investigated.

As in previous reports, we employed membrane integrity-based measurement following FDA / PI double staining to quantify the morphological survival of islet preparations [77–79]. However, a methodological limitation of this assay (2D analysis of 3D structure) has been raised [49, 80]. Therefore, GSIS analysis was also performed to evaluate the function of cryopreserved islets. The functional restoration of cryopreserved islets was assessed by SI value in the GSIS assay (**Table 2-2**). There are no distinct SI criteria to distinguish functional and dysfunctional islets, because glucose concentration for stimulation varies from 15 to 33 mM. Nevertheless, islets with an SI value larger than 3 have been empirically regarded as those maintaining functional insulin secretion and recommended for transplantation [81]. SI values of rat islets cryopreserved by Cryotop[®] vitrification were 3.9 and 3.1 at 0 and 24 h after warming, without statistical significance from the fresh control values. Increased basal insulin secretion level in islets

cryopreserved by Bicell[®] freezing may be responsible for the low SI values (< 2.0). Impaired glucose-responsiveness due to the high basal level in cryopreserved islets agrees with the findings in previous reports [51, 72]. Such an insulin leak is probably the result from islet death by cell rupture or necrosis. The qPCR analysis indicated that both *Pdx1* and *Glut2* less expressed in the frozen-thawed islets (**Fig. 2-4**), which can explain their impaired glucose uptake and the resultant inadequate GSIS response of β -cells regardless of comparable survival with the vitrified-warmed islets. However, it remains unclear how the Bicell[®] freezing protocol altered the upstream *Pdx1* expression.

Perfusion of rat pancreas with liberase solution resulted in the harvest of isolated islets (280.2 islets per rat, n=6) with various sizes (small: 101–200 μm , 68.5% / middle: 201–300 μm , 27.6% / large: > 300 μm , 3.9%) (data not shown). Therefore, an additional experiment was designed to investigate whether the original Cryotop[®] vitrification protocol can be applied to larger islets. Results indicated that > 150- μm islets were sensitive to vitrification and warming as far as the SI values were used for evaluation (**Fig. 2-5**). Insufficient permeation of CPA and/or suboptimal cooling rate in the larger size islets may result in dysfunction of insulin secretion, even though these phenomena were not detrimental for morphological survival. Similarly, von Mach *et al.* [82] reported a significant size-dependent negative correlation ($r < -0.8$) with cryosurvival of rat islets under a slow freezing regimen in DMSO solution. Sakonju *et al.* [75] also reported that, based on beta granule population, small size rat islets (< 200 μm) were more tolerant to two-step freezing regimen in DMSO or EG solution when compared with middle (200–300 μm) and large size (> 300 μm) islets. No publication is available for correlation between islet size and tolerance to vitrification, but Cryotop[®] vitrification protocol may not allow the wide size range of rat islets.

In conclusion, rat pancreatic islets can be cryopreserved by Cryotop[®] vitrification protocol rather than Bicell[®] freezing protocol, without considerable loss of β -cell function (insulin secretion) and gene expression (*Pdx1* and *Glut2*). Both SI values immediately after warming and after an additional 24 h culture exceeded 3.0, a recommended minimum value for islet transplantation.

2.5. Abstract

Cryopreservation of pancreatic islets without functional loss can overcome the inevitable shortage of donors and allow time to investigate immunological tissue matching between donors and recipients. The aim of the first study was to determine the optimal cryopreservation protocol for rat pancreatic islets. In the first study, two protocols, Bicell[®] freeze-thawing and Cryotop[®] vitrification-warming, were compared for suitability in cryopreserving rat pancreatic islets (101–150 μm in mean diameter). Immediate survival rates of post-thaw and post-warm islets (50 and 57%, respectively), assessed by FDA / PI double staining, were lower than that of fresh control islets (90%). Most of the PI-positive dead cells were detected in the peripheral area of post-warm islets, and were removed after subsequent 24 h culture (survival rate; 85 *versus* 59% in post-thaw islets). Quantitative PCR analysis showed that Bicell[®] freeze-thawing compromised expression of genes relating to β -cell function (*Pdx1* and *Glut2*), but not to one of the apoptotic pathways (*Bax* / *Bcl2* ratio). Expression of these genes was maintained in islets before and after the Cryotop[®] vitrification-warming. Values of stimulation index (SI) for 20 mM / 3 mM GSIS assay were 6.7, 1.9 and 3.9 in fresh control, post-thaw and post-warm islets, respectively. The SI values after 24 h culture were 4.1, 1.9 and 3.1, respectively. Larger islets (> 150 μm in diameter) had comparable survival rates, but lower SI values after Cryotop[®] vitrification-warming when compared to smaller counterparts. These results suggest that rat pancreatic islets can be cryopreserved by Cryotop[®] vitrification-warming rather than Bicell[®] freeze-thawing, without considerable loss of *in vitro* β -cell function.

Chapter 3 Nylon mesh device for vitrification of large quantities of rat islets

3.1. Introduction

Conventional cell freezing protocols have been employed for islet cryopreservation in rats and humans [48–50]. While a freezing protocol is advantageous because a large quantity of isolated islets can be handled with a relatively simple procedure, the inevitable formation of ice crystals may lead to impaired insulin secretion function of freeze-thawed islets [51–53]. This dysfunction in post-thaw islets results in the requirement of transplanting more than double the IEQ, compared with fresh islets, to achieve normoglycemia [49, 52]. Although attempts at cryopreserving the islets by vitrification resulted in a recovery of functional islets [56, 57], a considerable loss in post-warm islet viability and insulin secretion has been reported [58, 59]. Contrastingly, a vitrification protocol, which can avoid ice crystal formation by use of an extremely high cooling-warming velocity, is superior to conventional freezing in terms of GSIS and the expression of β -cell function-associated genes [83]. Different devices such as Cryotop[®] [83], open-pulled straw [68], and hollow fiber [84] have been employed for the vitrification of isolated rodent islets. However, vitrification protocols have a technical limit as large quantities of islets cannot be loaded onto or into each device (recommended quantity 10–12, possible upper limit 20–30).

Matsumoto *et al.* [65] reported that as many as 65 bovine immature COCs could be vitrified-warmed using nylon mesh as cryodevice, with subsequent work by Abe *et al.* [66] successfully producing a calf from these COCs. Because of the similar size characteristics between COCs and pancreatic islets, the present study was conducted to investigate the capacity of a nylon mesh device for vitrification of large quantities of rat pancreatic islets.

3.2. Materials and Methods

Experimental design

Rat pancreatic islets (size category: 101–151 μm $n = 10$ or 50) were subjected to one of three cryopreservation protocols (Cryotop[®] vitrification, nylon mesh vitrification, or Bicc[®] freezing) in a single replicate, and their post-warm / post-thaw survival rates were assessed by FDA / PI double staining. The SI values were measured with an ELISA kit for functional analysis in vitro. Nylon mesh was selected as the cryodevice for the larger number of islets (10, 50 and 100 islets per single operation). The survival and SI values of the vitrified-warmed islets were measured to determine whether the nylon mesh enabled the scale-up of islet numbers in a single operation.

Chemicals and animals

Unless otherwise indicated, chemicals used in the present study were purchased from Sigma-Aldrich. The SPF-graded BN rats were purchased from Japan SLC. Rats were housed in an environmentally controlled room with a 12-h dark / 12-h light cycle at a temperature of $23 \pm 3^\circ\text{C}$, with free access to a laboratory diet (NMF; Oriental Yeast) and tap water. All experimental animal procedures were reviewed and approved by the Animal Care and Use Committee of the Shinshu University, Nagano, Japan. Animals were treated humanely and the standards conformed to those of current ethical animal research practices.

Isolation of rat islets

Pancreatic islets were isolated from male rats at 8–12 weeks old. Briefly, the bile duct of the rats was cannulated with a fine plastic tube and the pancreas was distended with approximately 8 mL of liberase TL solution (1 WU/mL liberase in cold HBSS). The pancreas was excised, minced, and incubated at 37°C for 30 min, and then the digested tissues were purified on a discontinuous histopaque gradient that was layered with histopaque1119, histopaque1077, and 2% FBS in HBSS. Islets with a size of 101–150 μm in mean longest and widest diameter were handpicked using capillary pipettes under a stereomicroscope, and cultured for 24 h in 2 mL of RPMI-1640 supplemented with 10% FBS and antibiotics (100 units/mL

penicillin and 100 µg/mL streptomycin) at 37°C in a humidified atmosphere of 5% CO₂ in air until use for cryopreservation.

Cryopreservation

The Cryotop[®] vitrification protocol was conducted as described previously [83]. Briefly, islets were equilibrated with 7.5% EG (Wako) and 7.5% DMSO (Wako) in RPMI-1640 supplemented with 20% FBS for 3 min at ambient temperature ($25 \pm 2^\circ\text{C}$), and then transferred into a VS comprising 15% EG, 15% DMSO, and 0.5 M sucrose as CPAs in RPMI-1640 containing 20% FBS for 60 sec at ambient temperature. Within this 60-sec period, 10 islets were loaded onto the polypropylene strip of a Cryotop[®] device (Kitazato) with a minimal volume of the VS, and then quickly plunged into LN₂. After storage for at least 1 week, islet warming was performed by immersing the polypropylene strip of Cryotop[®] into RPMI-1640 containing 20% FBS and 1 M sucrose at 38.5°C for 1 min. Following warming, islets were transferred to RPMI-1640 containing 20% FBS and sucrose in a stepwise manner (0.5, 0.25, and 0 M sucrose for 3, 5, and 5 min, respectively).

The Nylon mesh vitrification protocol was conducted as described previously [66], with some modifications to enable the original protocol developed for bovine COCs to be adapted to rat islets. Briefly, a 10-mm triangle sheet was cut from commercially available nylon mesh (pore size $\phi = 57 \mu\text{m}$; Sansyo Co., Ltd., Tokyo, Japan) and processed to form a triangular pyramid by folding into quarters (**Fig. 3-1 A**). Islets were equilibrated with 7.5% EG and 7.5% DMSO in RPMI-1640 containing 20% FBS for 3 min at ambient temperature, and then placed onto the center triangle of the sterilized nylon mesh device using a capillary pipette. Immediately thereafter the equilibration solution was removed by placing the device on a sterilized filter paper (Kimwipes[®]; Nippon Paper Crexia Co., Ltd., Tokyo, Japan), and the islets on the device were exposed to VS (15% EG, 15% DMSO, and 0.5 M sucrose in RPMI-1640 containing 20% FBS) for 60 sec at ambient temperature using sterilized tweezers. Within this 60-sec period, the device was placed on new sterilized Kimwipes[®] and then quickly plunged into LN₂. After storage in LN₂-filled 50-mL conical tubes at least for 1 week, islet warming was performed by immersing the device into RPMI-1640 containing 20% FBS and 1 M sucrose at 38.5°C for 1 min. Following warming, islets on the device were transferred to RPMI-1640 containing 20% FBS and sucrose

in a stepwise manner (0.5, 0.25, and 0 M sucrose for 3, 5, and 5 min, respectively). Islets were released from the device during the last 5-min exposure to the sucrose-free solution by using a capillary pipette. A schematic diagram of the nylon mesh vitrification protocol is shown in **Fig. 3-1 B to D**.

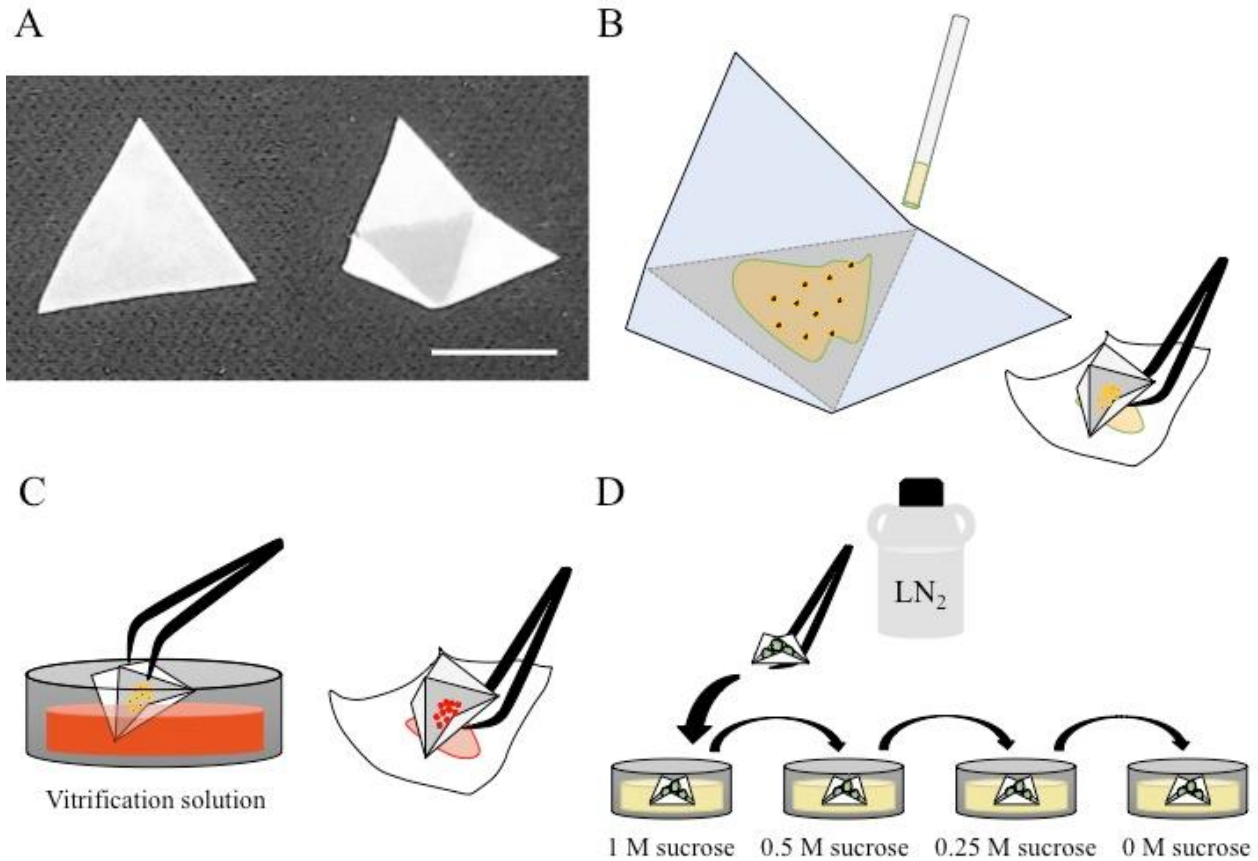


Fig. 3-1. Outline of islet vitrification with nylon mesh device. (A) Nylon mesh device, a developed figure of a triangular pyramid. Scale bar = 5-mm. (B) After 3-min equilibration with permeable CPAs, the islets are placed on the center triangle of the device and the surrounding solution is removed with Kimwipes®. (C) The device is transferred to vitrification solution with tweezers, and then amount of the vitrification solution is minimized with Kimwipes®. (D) Stepwise removal of CPAs from post-warm islets can be performed on the device with tweezers, not glass capillary. Islets are warmed in 1 M sucrose solution, and then transferred to 0.5, 0.25, and 0 M sucrose solutions in a stepwise manner.

According to the manufacturer's instruction manual, a conventional freezing protocol was conducted using Bicell[®] bio freezing vessels (Nihon Freezer). Briefly, islets were exposed to 15% DMSO in RPMI-1640 containing 10% FBS and antibiotics for 15 min at ambient temperature, and then cooled to 4°C for 15 min. Fifty islets were placed in a precooled cryotube containing 500 µL of the above-mentioned CPA solution, and the cryotubes were packed into a Bicell[®] vessel. Subsequently, the Bicell[®] vessel was placed in a -80°C deep freezer overnight (estimated cooling rate, -0.5°C/min during the first 3 h), and then the cryotubes were transferred into LN₂. After storage for at least 1 week, the cryopreserved islets were thawed by gently warming the cryotubes in a 37°C water bath for 1 min. Following thawing, islets were transferred to RPMI-1640 containing 10% FBS, antibiotics, and sucrose in a stepwise manner (1.0, 0.5, 0.25, and 0 M sucrose for 2, 3, 5, and 5 min, respectively).

Survival assay

Islet survival was assessed by double staining with FDA and PI, as described previously [83]. An aliquot of 10 islets in each group was stained with 25 µg/mL FDA and 25 µg/mL PI for 30 sec in the dark. After three washes in PBS, micrographs depicting FDA (green) and PI (red) fluorescence were taken using an epifluorescence microscope (IX73; Olympus). The fluorescent area was quantified using Image J software. The survival rate was calculated as: $100 \times \text{FDA-positive area} / \text{total of FDA-positive} + \text{PI-positive area}$.

Insulin secretion

Islet functionality was assessed by static GSIS assay. Briefly, post-thaw / post-warm islets (10 each per group) were washed three times with RPMI-1640 containing 10% FBS and 3 mM glucose and incubated for 1 h at 37°C in a humidified atmosphere of 5% CO₂ in air. The islets were then stimulated by transfer into RPMI-1640 containing 10% FBS and 20 mM glucose and incubated for 1 h as described above. At the end of incubation, supernatants were collected and stored at -80°C until an insulin assay was conducted. The basal and stimulated insulin levels (ng/islet/h) were determined using an ELISA kit for rat insulin (MioBS), and the SI was defined as the stimulated insulin level in response to 20 mM glucose divided by the basal level in response to 3 mM glucose.

Statistical analysis

Percentage data were subjected to arcsine transformation before statistical analysis. Differences between groups were assessed by one-way ANOVA. When ANOVA was significant, differences among values were analyzed by Tukey's Honest Significant Difference test for multiple comparisons. Data were considered statistically significant at $p < 0.05$.

3.3. Results

Cryosurvival and insulin secretion

All islets cryopreserved were recovered after thawing/warming (100% recovery). Survival of frozen-thawed islets (Bicell[®] group) was significantly lower than that of vitrified-warmed islets (both Cryotop[®] and Nylon mesh groups), as shown in **Fig. 3-2**. While the insulin secretion level in response to 3 mM glucose was higher in frozen-thawed versus vitrified-warmed islets, the insulin secretion levels stimulated by 20 mM glucose were comparable among the three groups, as shown in **Table 3-1**. Therefore, the SI value for the Bicell[®] group (0.8) was significantly lower or tended to be lower than values for the Cryotop[®] and Nylon mesh groups (3.9 and 3.1, respectively). For reference, non-cryopreserved fresh islets were isolated from the same donor rat colony, with a survival rate of $92.1 \pm 1.5\%$ and an SI value of 7.3 ± 0.8 (4 replicates) obtained.

Islet scale effect

Both the exposure of islets to VS before cooling and the stepwise CPA dilution of post-warm islets were achieved without using glass capillaries to maintain a tight time schedule for each step (**Fig. 3-1**). Almost all islets were recovered after nylon mesh vitrification/warming in a unit of 10 islets (100%, 160/160), 50 islets (99.3%, 397/400), and 100 islets (98.9%, 791/800). Only a few periphery layers of islet cells are likely to be damaged by vitrification (**Fig. 3-3**). Small debris located in the periphery of post-warm islets after CPA dilution disappeared within a few hours of recovery culture. When the number of islets loaded onto a nylon mesh device increased from 10 to 50 or 100, the survival rate of vitrified-warmed islets did not change

significantly, as shown in **Fig. 3-4**. Additionally, the number of samples per device did not affect GSIS in the post-warm islets, which was within the normal range (SI 2.8–4.2), as shown in **Table 3-2**.

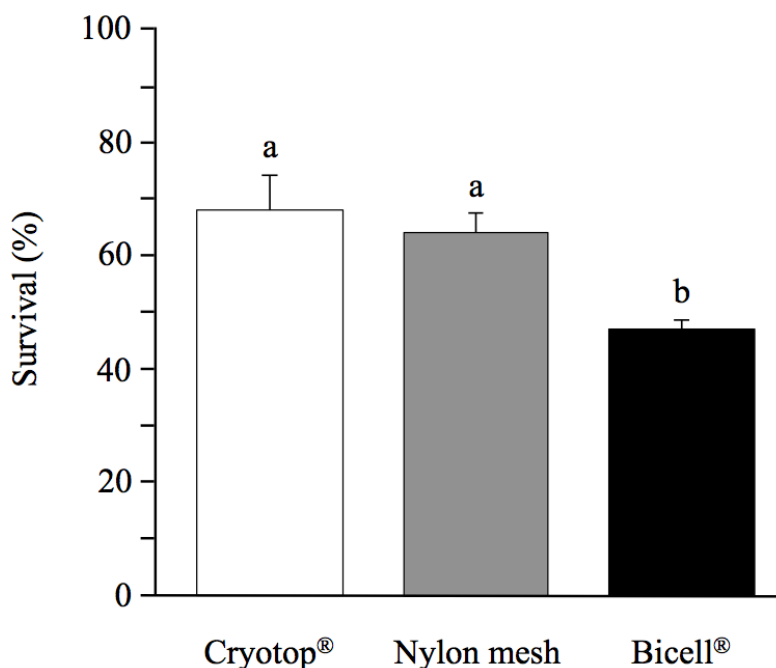


Fig. 3-2. Survival of islets cryopreserved by Cryotop® vitrification, nylon mesh vitrification or Bicell® freezing. Data are expressed as the mean \pm SEM of 6 replicates in each group. ^{a,b} Different superscripts represent significantly different groups ($P < 0.05$).

Table 3-1. GSIS from cryopreserved rat islets.

Group	3 mM glucose (ng/islet/h)	20 mM glucose (ng/islet/h)	Stimulation index
Cryotop®	0.18 \pm 0.06 ^a	0.45 \pm 0.07	3.9 \pm 1.2 ^a
Nylon mesh	0.15 \pm 0.03 ^a	0.42 \pm 0.09	3.1 \pm 0.7 ^{ab}
Bicell®	0.61 \pm 0.08 ^b	0.54 \pm 0.15	0.8 \pm 0.2 ^b

Data are expressed as the mean \pm SEM of 6 replicates in each group.

^{a,b} Different superscripts represent significantly different groups ($P < 0.05$).

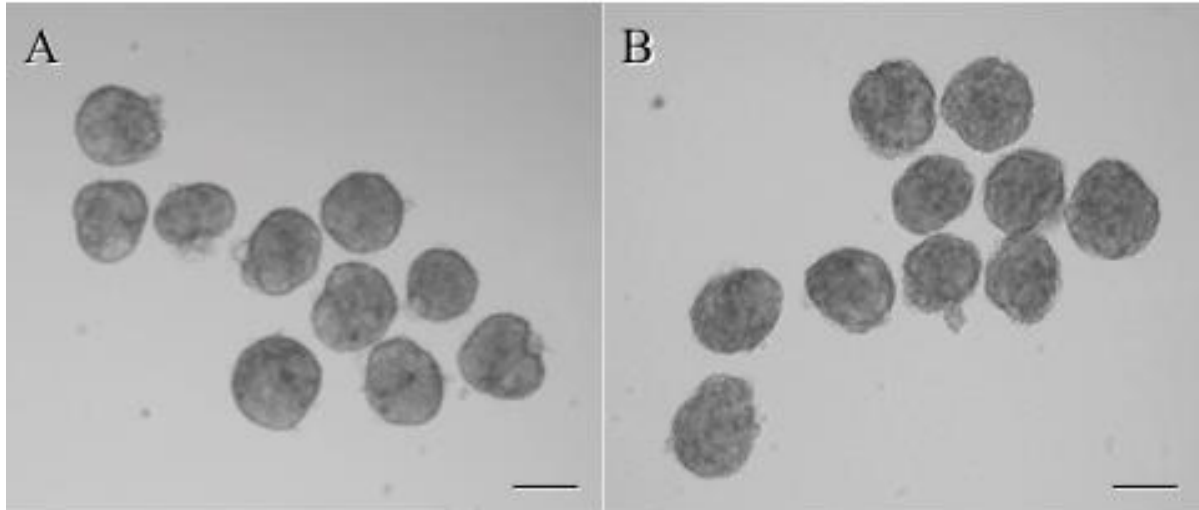


Fig. 3-3. Morphology of rat islets vitrified-warmed using a nylon mesh device. (A) Fresh control islets. (B) Post-warm islets recovered from the device after stepwise CPA dilution. Only a few periphery layers of islet cells are likely to be damaged by vitrification. Scale bars = 100- μ m.

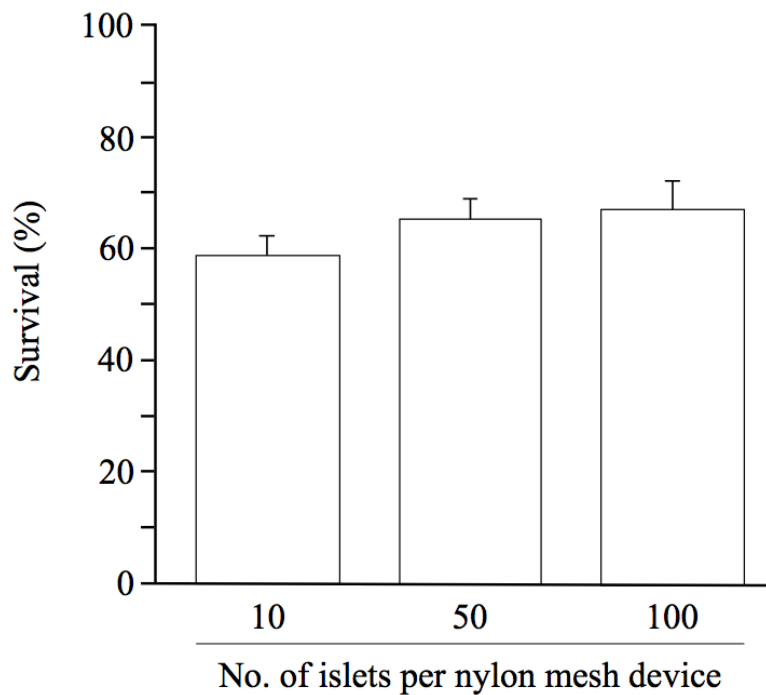


Fig. 3-4. Effect of sample size per nylon mesh device on the survival of vitrified-warmed rat islets. Data are expressed as the mean \pm SEM of 8 replicates in each group. No significant differences were detected among three groups.

Table 3-2. Effect of sample size per nylon mesh device on the GSIS of vitrified-warmed rat islets.

Islet no.	3 mM glucose (ng/islet/h)	20 mM glucose (ng/islet/h)	Stimulation index
10	0.12 ± 0.02	0.50 ± 0.12	4.2 ± 0.4
50	0.17 ± 0.05	0.61 ± 0.15	3.8 ± 0.5
100	0.11 ± 0.02	0.28 ± 0.04	2.8 ± 0.5

Data are expressed as the mean ± SEM of 8 replicates in each group.

No significant differences were detected among three groups.

3.4. Discussion

Using nylon mesh devices for the vitrification of rat pancreatic islets overcomes the technical scale limit faced by some cryodevices during islet cryopreservation [68, 83, 84]. We successfully employed the same pre- and post-vitrification CPA treatments reported previously for Cryotop[®] vitrification [83] during nylon mesh vitrification, as assessed by cryosurvival and GSIS (**Fig. 3-2** and **Table 3-1**). The Cryotop[®] vitrification protocol has been recommended over the Bicell[®] freezing protocol [83], despite of injurious aspect of highly concentrated CPAs. However, the Cryotop[®] vitrification protocol may be unsuitable for large-scale operation (> 30 islets per device) because necessary treatments —such as CPA equilibration, VS exposure, VS minimization, and CPA dilution— are difficult to achieve within the required timeframe. Dysfunctional islets were recovered from conventional Bicell[®] freezing, despite the capacity for cryopreservation of large quantities of pancreatic islets, as reported previously [68, 83, 84].

Practically acceptable levels of cryosurvival and SI were obtained after scaling up to 100 islets per nylon mesh device (**Fig. 3-4** and **Table 3-2**). This suggests that the nylon mesh device offers promising advantages including easy handling of large quantities of islets and minimization of VS volume for ultra-rapid cooling/warming (**Fig. 3-1**). Recently, this concept of the nylon mesh vitrification has been successfully extended to > 40 in vitro-matured bovine oocytes, with

improved cryosurvival by applying the smaller $\phi = 37\text{-}\mu\text{m}$ nylon mesh pore [85] and the resveratrol treatment to post-warm oocytes [86]. The effectiveness of islets cryopreserved for the longer period of time remained to be examined from a viewpoint of practical importance. The solid surface vitrification (SSV) protocol, which was originally developed in bovine COCs [87], allows cryopreservation of large quantities of islets (100 islets per 40- μL microdrop) [68]. However, islet handling with glass capillaries may be time-consuming and labor intensive. The hollow fiber vitrification (HFV) protocol has been used for mouse, porcine, and bovine embryos [88–90], and for mouse islets [84]. The HFV protocol simplifies the processes of CPA addition/dilution because of the microdialyzable characteristics of the hollow fiber device, and has been applied to a maximum of 40 mouse embryos [87] or 25–35 islets [84] in a single device.

The SI values (20 mM / 3 mM glucose) of rat islets vitrified with nylon mesh device ranged from 2.8 to 4.2 (**Tables 3-1, 3-2**). Sasamoto *et al.* [68] reported that the SI value of vitrified rat islets in the original SSV protocol was only 1.1, and that modification in the VS composition (EDT324; composed from 30% EG, 20% DMSO and 0.4 M trehalose) increased the SI value up to 6.4. Additionally, Nagaya *et al.* [84] failed to demonstrate the SSV suitability with the EDT324 solution for mouse islets, but reported an SI value (28 mM / 2.8 mM glucose) of 3.5 when the HFV protocol was applied. The islet insulin secretion potential measured *in vitro* is closely related to the *in vivo* response for glycemic control [49, 68]. Increasing the islet number per nylon mesh device (from 10 to 100) resulted in a mild increase in cryosurvival (from 59 to 69%; **Fig. 3-4**) and a decrease in SI (from 4.2 to 2.8; **Table 3-2**), requiring IEQ-based further investigation for the presence and significance of a negative correlation.

In conclusion, nylon mesh can serve as cryodevice for the vitrification of large quantities of rat pancreatic islets under the practical requirement for handling the higher amount of islets in a single operation. Such nylon mesh vitrification is practically advantageous because islets can be handled for CPA addition/dilution without glass capillary micro-pipetting under a strictly controlled timetable. It remains for further investigations to develop vitrification regimens optimal for the larger size islets and to confirm the adaptability of vitrified-warmed islets to cure hyperglycemia of diabetes model rats by islet transplantation.

3.5. Abstract

The practical requirements of islet transplantation necessitate that a large quantity of pancreatic islets is cryopreserved for a long period of time in a simple and convenient manner. In the present study, 101–150 μm -sized islets were cryopreserved by vitrification with either a Cryotop[®] device or a $\varnothing = 57\text{-}\mu\text{m}$ nylon mesh device in units of 10 islets, or by conventional freezing with a Bicell[®] vessel in units of 50 islets. Post-warm / post-thaw survival rates of the islets were 68, 64, and 48% following Cryotop[®] vitrification, nylon mesh vitrification, and Bicell[®] freezing, respectively. GSIS in the two vitrification groups (SI values = 3.1–3.9) was superior to that in the freezing group (SI value = 0.8). Additional experiments involved scaling-up the cryopreservation process using the nylon mesh device in units of 10, 50, or 100 islets. Increased numbers of islets per device had no adverse effects on cryosurvival (59–69%) or insulin secretion potential (SI values = 2.8–4.2). As the nylon mesh device does not require the handling of individual islets with glass pipettes, pre- and post-vitrification islet treatment is less complicated. Therefore, nylon mesh can serve as a simple cryodevice for the vitrification of large quantities of rat pancreatic islets, with the post-warm functional insulin secretion potential.

Chapter 4 Glycemic control by subrenal transplantation of vitrified rat islets

4.1. Introduction

Islet transplantation is considered as a useful option for the clinical treatment of T1D patients since the Edmonton protocol has been established in 2000 [20]. However, many T1D patients require multiple transplantation treatments to maintain the therapeutic effect as insulin independence [39, 40]. Considerable loss of transplanted islets occurs due to an IBMIR [43, 44]. Therefore, a huge number of islets (10,000–12,000 IEQ/kg recipient body weight) must be prepared from multiple donor pancreata for single islet intra-hepatic transplantation via portal infusion [20, 42]. In the rodent model system, 150–300 islets per recipient mouse [47, 91–96] or 800–1,200 islets per recipient rat [47, 97–101] have been used to cure the streptozotocin (STZ)-induced diabetes by subrenal transplantation. As rat islets seemed to be dysfunctional after conventional freezing and thawing, more than double post-thaw islets were required to restore normoglycemia by their transplantation compared to the non-frozen fresh islets [49, 52]. In a freeze-thawing experiment of mouse islets using taurine, 500 IEQ transplantation rescued diabetic mice, while 250 IEQ was a suboptimal dose [102]. When vitrification-warming procedures were applied to islet cryopreservation, 300 mouse post-warm islets [84] or 800 rat post-warm islets [66] per recipient have been used to achieve normoglycemia by subrenal transplantation.

Transplants comprised primarily of small rather than large islets may provide preferable graft function, because they are less susceptible to hypoxic damage. As to the size-dependent functional difference of isolated islets, a number of *in vitro* and *in vivo* studies have shown that smaller islets have superior function compared with larger ones. They include the higher insulin content [103, 104] or secretion [105–107] of small versus large islets, and better glycemic control by small versus large islet transplantation beneath kidney capsule [107, 108] or into a portal vein [109]. MacGregor *et al.* [107] reported in rats that small islets with a mean diameter

of 50.3 μm , compared to large islets with a mean diameter of 204 μm , showed higher performance in survival, oxygen consumption, GSIS and glycemic control of diabetic rats by subrenal transplantation. Lehmann *et al.* [110] reported in a clinical study that the better function was associated with grafts comprising of the smaller human islets (fresh source). We have previously reported that the smaller rat islets were more tolerant to vitrification injuries than the larger ones as compared by GSIS assay [83]. von Mach *et al.* [82] also reported a negative correlation between rat islet size and survival after cryopreservation by freeze-thawing.

In the present study, the adaptability of vitrified-warmed rat islets to cure hyperglycemia of diabetic rats was investigated by syngeneic subrenal transplantation. Small and/or middle size BN rat islets cryopreserved by vitrification using nylon mesh device were transplanted beneath the kidney capsule of the STZ-induced diabetes model BN rats.

4.2. Materials and Methods

Experimental design

In a preliminary experiment, rat pancreatic islets were first classified into one of three size categories (small 101–150 μm ; medium 151–200 μm ; large 201–250 μm), cultured for 24 h, and then were assessed for survival by FDA / PI double staining and insulin secretion potential by ELISA. Then, in the main experiment, rat islets (small + medium size category: 101–200 μm , $n = 100$ per device) were cryopreserved by a vitrification protocol using nylon mesh device, as described previously [111]. The post-warm islets, as well as fresh control islets ($n = 800$ per recipient), were surgically transplanted beneath the kidney capsule of the STZ-induced diabetic rats, and the blood glucose levels of the recipients were monitored. Cured recipients were subjected to intraperitoneal glucose tolerance test (IPGTT) 30 and 60 days after the islet transplantation. Reversal of hyperglycemia following nephrectomy indicates normal *in vivo* functionality of transplanted islets, confirmed further by histology of engrafts stained with hematoxylin-eosin (H&E).

Chemicals and animals

Unless otherwise indicated, chemicals used in the present study were purchased from Sigma-Aldrich. The SPF-graded BN rats purchased from Japan SLC were housed in an environmentally controlled room with a 12-h dark/12-h light cycle at a temperature of $23 \pm 3^\circ\text{C}$, with free access to a laboratory diet (NMF; Oriental Yeast) and tap water. All experimental animal procedures were reviewed and approved by the Animal Care and Use Committee of the Shinshu University, Nagano, Japan. Animals were treated humanely and the standards conformed to those of current ethical animal research practices.

Isolation of rat islets

Pancreatic islets were isolated from male rats at 8–12 weeks old. Briefly, the bile duct of the rats was cannulated with a fine plastic tube and the pancreas was distended with approximately 8 mL of liberase TL solution (1 WU/mL liberase in cold HBSS). The pancreas was excised, minced, and incubated at 37°C for 30 min, and then the digested tissues were purified on a discontinuous histopaque gradient that was layered with histopaque1119, histopaque1077, and 2% FBS in HBSS. Islets with a size of 101–350 μm in mean longest and widest diameter were handpicked using capillary pipettes (inner diameter: 150, 200, 250, 300 or 350- μm) under a stereomicroscope, and cultured for 24 h in 2 mL of RPMI-1640 supplemented with 10% FBS and antibiotics (100 units/mL penicillin and 100 $\mu\text{g}/\text{mL}$ streptomycin) at 37°C in a humidified atmosphere of 5% CO_2 in air.

Vitrification and warming

The Nylon mesh vitrification protocol was conducted as described previously [111], with a modification in mesh pore size [85]. A 10-mm triangle sheet was cut from commercially available nylon mesh (pore size $\phi = 37 \mu\text{m}$) and processed to form a triangular pyramid by folding into quarters. Islets were equilibrated with 7.5% EG and 7.5% DMSO in RPMI-1640 containing 20% FBS for 3 min at ambient temperature, and then placed onto the center triangle of the sterilized nylon mesh device using a capillary pipette. Immediately thereafter the equilibration solution was removed by placing the device on a sterilized filter paper (Kimwipes[®]), and the islets on the device were exposed to VS (15% EG, 15% DMSO, and 0.5 M sucrose in RPMI-1640

containing 20% FBS) for 60 sec at ambient temperature using sterilized tweezers. Within this 60-sec period, the device was placed on new sterilized Kimwipes[®] and then quickly plunged into LN₂. After storage in LN₂-filled 50-mL conical tubes at least for 1 week, islet warming was performed by immersing the device into RPMI-1640 containing 20% FBS and 1 M sucrose at 38.5°C for 1 min. Following warming, islets on the device were transferred to RPMI-1640 containing 20% FBS and sucrose in a stepwise manner (0.5, 0.25, and 0 M sucrose for 3, 5, and 5 min, respectively). Islets were released from the device during the last 5-min exposure to the sucrose-free solution by using a capillary pipette.

In vitro assays for islet survival and insulin secretion

Islet survival was assessed by double staining with FDA and PI as described previously [83]. An aliquot of 10 islets in each group was stained with 25 µg/mL FDA and 25 µg/mL PI for 30 sec in the dark. After three washes in PBS, micrographs depicting FDA (green) and PI (red) fluorescence were taken using an epifluorescence microscope. The fluorescent area was quantified using Image J software.

Islet functionality was assessed by static GSIS assay. Islets (10 each per size category) were washed three times with RPMI-1640 containing 10% FBS and 3 mM glucose and incubated for 1 h at 37°C in a humidified atmosphere of 5% CO₂ in air. The islets were then stimulated by transfer into RPMI-1640 containing 10% FBS and 20 mM glucose and incubated for 1 h as described above. At the end of incubation, supernatants were collected and stored at -80°C until an insulin assay was conducted. The basal and stimulated insulin levels (ng/islet/h or ng/IEQ/h) were determined using an ELISA kit for rat insulin.

Islet transplantation

Diabetes model rats were prepared by a single intravenous injection of STZ (Wako) at the dose of 65 mg/kg to male BN rats at 8–12 weeks old. Six days after the STZ injection, blood was collected from the tail vein, and non-fasting blood glucose level was monitored with a glucometer (Glucocard[™] G Black; Arkray, Inc., Kyoto, Japan). Rats were considered diabetic with a blood glucose level of > 350 mg/dL, and were subjected to islet transplantation the next day.

On the day of islet transplantation (defined as Day-0), the diabetic rats were anesthetized

with inhalation of isoflurane gas and intramuscular injection of medetomidine hydrochloride (1.2–2.5 mg/kg; Kyoritsu Seiyaku Co., Tokyo, Japan) and butorphanol tartrate (0.8–1.7 mg/kg; Meiji Seika Pharma Co., Ltd., Tokyo, Japan), and the skin was shaved and swabbed with iodophors. The left kidney was exposed through a lumbar incision (**Fig. 4-1 A**). Eight hundred islets (size category: 101 to 200 μm in diameter) in fresh control group or nylon mesh vitrification group were transplanted into the space beneath the renal capsule of the diabetic rats, using a glass capillary connected to the mouthpiece. The islet graft was visible over the capsule as white spot clusters (**Fig. 4-1 B**). The capsulotomy was left unsutured. The kidney was placed back into its original position and the incision was closed with a surgical suture. Un-fasting blood glucose

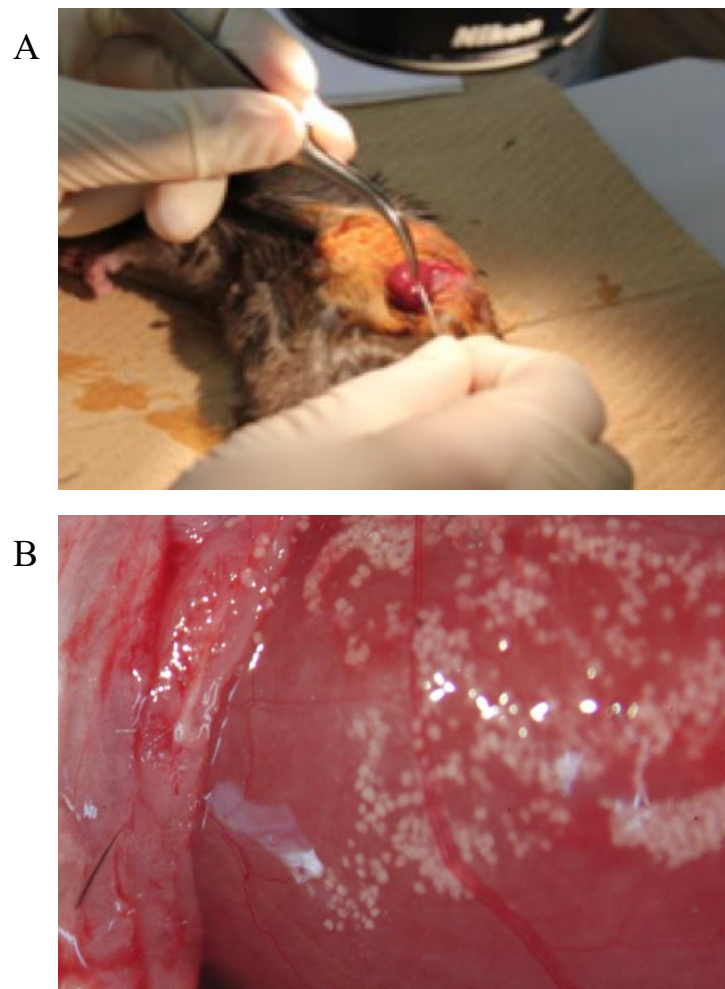


Fig. 4-1. Subrenal islet transplantation. (A) Kidney is exposed under an anatomical microscope. (B) Islet clusters (white spots) injected beneath the kidney capsule.

level, sampled by tail puncture, and body weight gain of the recipient rats were monitored on Day-1, -4, -7, -14, -21, -28, -35, -42, -49, -56, -63, and -70 to assess islet graft function. Rats that maintained < 200 mg/dL blood glucose level for two consecutive measurements were considered to have reversed diabetes (normoglycemia). The left kidneys containing islet grafts of the cured rats were removed on Day-70 under isoflurane anesthesia, and blood glucose level and body weight of the hemi-nephrectomized rats were monitored on Day-71, -74, and -77.

Engrafts from the nephrectomized rats were evaluated for morphological characterization. Briefly, the Day-70 kidneys with islet grafts were fixed in 4% PFA / PBS and kept at 4°C until use. They were transferred to 70% ethanol and processed to the paraffin-embedded tissue block. Each paraffin block was then sectioned into 4 µm in thickness. The sections were deparaffinized in Hemp-De® (Falma Co., Ltd., Tokyo, Japan), rehydrated through a series of ethanol to water and stained with H&E using a Leica Autostainer XL (Leica Microsystems, Wetzlar, Germany). The sections were rinsed in water and ethanol, cleared in the Hemp-De®, and mounted with coverslips in the Malinol (Muto Pure Chemicals Co., Ltd., Tokyo, Japan).

Intraperitoneal glucose tolerance test (IPGTT)

To conduct the IPGTT for the further assessment of the metabolic capacity of the islet grafts, the cured rats were fasted overnight before receiving an intraperitoneal glucose bolus (2 g/kg; administered as a 50% solution in water) on Day-30 and -60. Blood glucose levels, sampled by tail puncture, were monitored at baseline (time 0, 15, 30, 60, and 120 min) after injection, allowing for the area under the curve (AUC) to be calculated and analyzed between the fresh control group and nylon mesh vitrification group.

Statistical analysis

Percentage data were subjected to arcsine transformation before statistical analysis. Differences between groups were assessed by one-way ANOVA. When ANOVA was significant, differences among values were analyzed by Tukey's Honest Significant Difference test for multiple comparisons. Data were considered statistically significant at $P < 0.05$.

4.3. Results

To understand islet size variation, a total of 1,681 islets with 101–350 μm in diameter were isolated from 5 donor rats. Islets classified into three size categories (small 101–150 μm ; medium 151–200 μm ; large 201–250 μm) occupied 85.6% of the total islets isolated (**Fig. 4-2**).

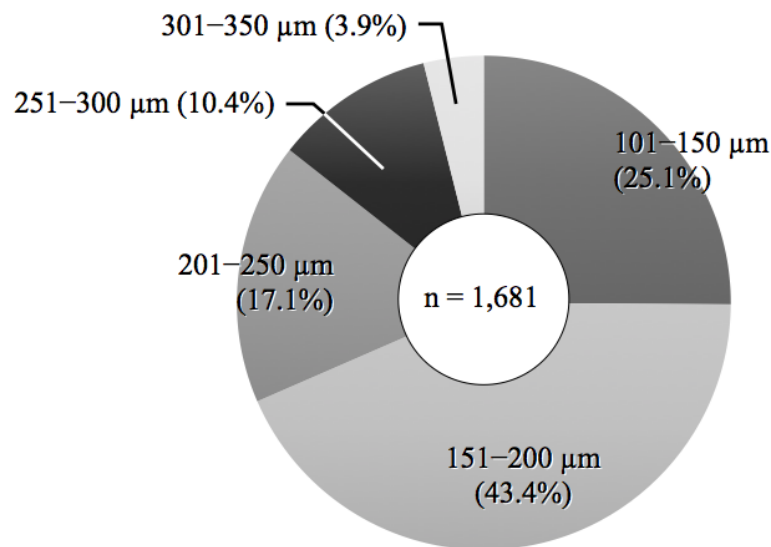


Fig. 4-2. Size distribution of pancreatic islets isolated from five BN male rats (ranged from 101 to 350 μm in mean diameter).

After 24-h culture, islet survival rates were comparable among size category groups (ranged 92.5 to 99.0%; **Table 4-1**). The GSIS assay indicated that insulin secretion after high (20 mM) glucose stimulation increased significantly in a size-dependent manner. On the other hand, when these insulin secretion levels per islet were converted to those per IEQ, the levels were negatively correlated to the size category both after low (3 mM) and high (20 mM) glucose stimulations. The SI values were comparable among the three groups (ranged from 7.22 to 9.58).

The recovery rate of islets vitrified-warmed using nylon mesh device was 97.1% (5,550/5,715). As shown in **Table 4-2**, the cryosurvival rate of the post-warm islets was significantly lower than that in the fresh control group. The GSIS assay of the post-warm islets indicated a significant difference between fresh control and vitrification groups in response to 3 mM glucose, but no difference in the SI value (**Table 4-2**).

Table 4-1. Survival and GSIS of rat islets with different size category.

Size category	Survival (%)		Insulin secretion (ng/h)		Stimulation index
			3 mM glucose	20 mM glucose	
Small (101–150 μ m)	96.9 \pm 1.5	Per islet	0.031 \pm 0.005	0.208 \pm 0.019 ^a	7.22 \pm 1.22
		Per IEQ	0.045 \pm 0.007 ^x	0.303 \pm 0.027 ^x	
Medium (151–200 μ m)	92.5 \pm 2.9	Per islet	0.035 \pm 0.004	0.322 \pm 0.018 ^b	9.58 \pm 0.74
		Per IEQ	0.026 \pm 0.004 ^y	0.242 \pm 0.012 ^{xy}	
Large (201–250 μ m)	99.0 \pm 0.4	Per Islet	0.049 \pm 0.006	0.443 \pm 0.027 ^c	9.40 \pm 0.82
		Per IEQ	0.022 \pm 0.003 ^y	0.200 \pm 0.014 ^y	

Data are expressed as the mean \pm SEM of 5 replicates in each category.

^{a-c, x,y} Different superscripts within a column represent significantly different groups ($P < 0.05$).

Table 4-2. Survival and GSIS of post-warm rat islets used for subrenal transplantation.

Groups	Survival (%)	Insulin secretion (ng/islet/h)		Stimulation index
		3 mM glucose	20 mM glucose	
Fresh control	97.5 \pm 0.5 ^a	0.13 \pm 0.02 ^a	0.82 \pm 0.04	6.5 \pm 0.6
Vitrification	77.9 \pm 3.0 ^b	0.26 \pm 0.05 ^b	1.06 \pm 0.06	4.7 \pm 0.7

^{a,b} Different superscripts within a column denote significant difference ($P < 0.05$).

Mean \pm SE, 5 replicates (survival), and 6 replicates (GSIS).

When the post-warm 800 islets were injected beneath the kidney capsule, 7 out of 8 recipients (87.5%) and 5 out of 6 recipients (83.3%) achieved normoglycemia in the fresh control group and vitrification group, respectively (**Fig. 4-3**). One each recipient rat that had not been rescued from hyperglycemia by islet transplantation was sacrificed on Day-28. Except for 1 recipient rat in vitrification group that died accidentally during Day-70 nephrectomy operation,

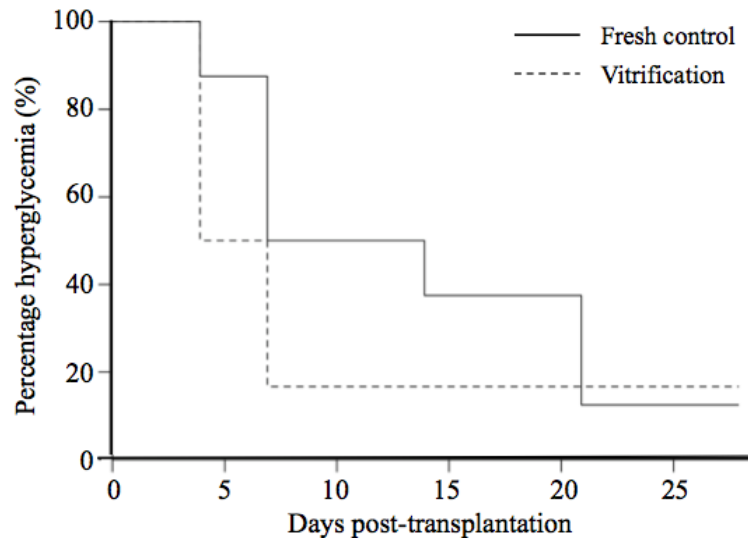


Fig. 4-3. A Kaplan-Meier plot for proportion of recipients that achieved normoglycemia following transplantation of fresh control and vitrified-warmed islets.

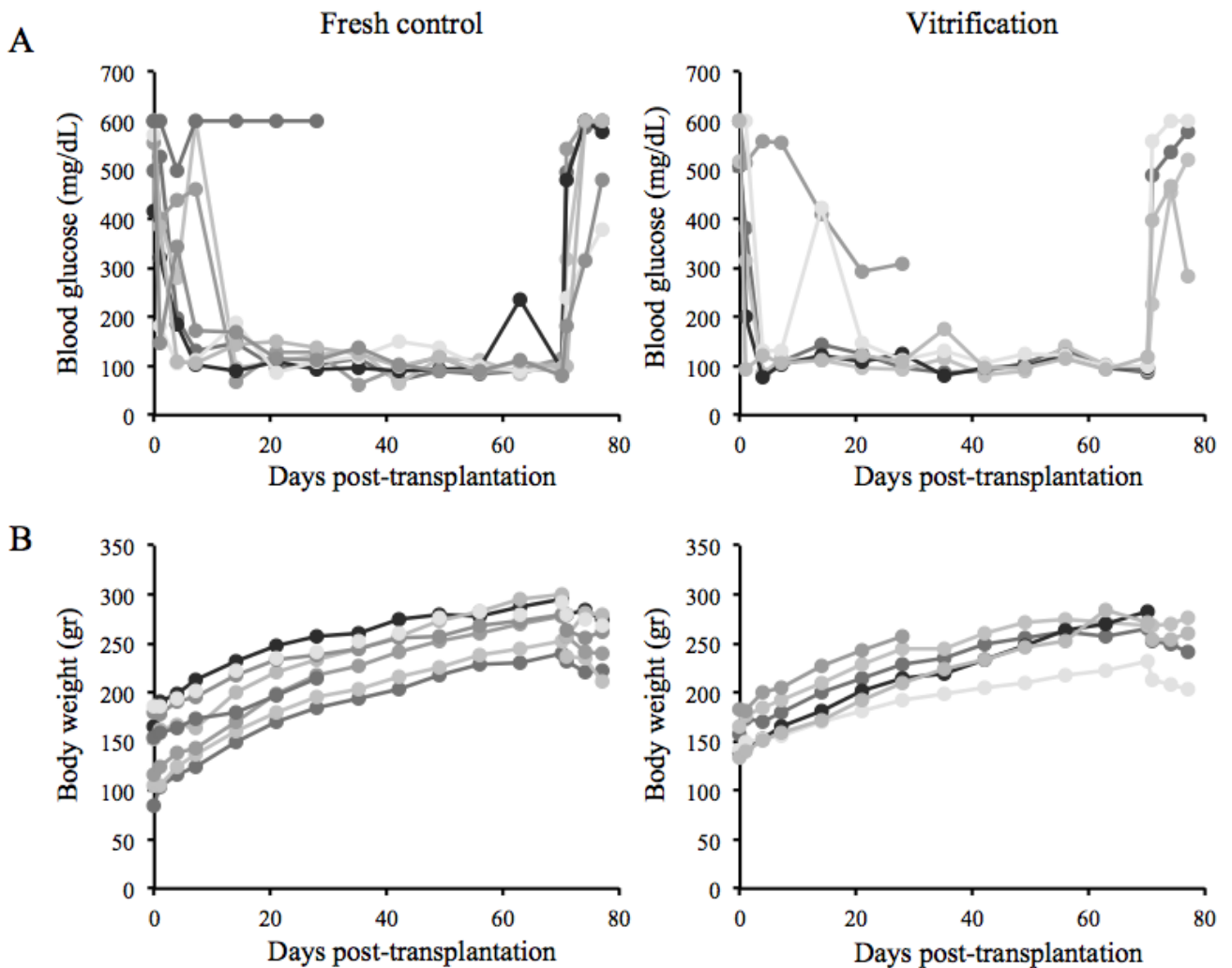


Fig. 4-4. Glycemic control of individual diabetic rats by syngeneic subrenal transplantation of fresh and vitrified-warmed islets. (A) Blood glucose level. (B) Body weight gain.

regained hyperglycemia of all 11 recipients after the nephrectomy reflected the normal function of transplanted islets (**Fig. 4-4 A**). Thus, possible natural healing of STZ-induced diabetes was neglected. Inhibited body weight gain after the nephrectomy of cured recipients (**Fig. 4-4 B**) may reflect their diabetic symptom, along with the effect of surgical operation. Islet engrafts with angiogenesis (**Fig. 4-5 A**) were recovered successfully from all the cured recipient rats. The proportion of blood vessel area per islet in the sections (**Fig. 4-5 B**) was 8.3% (Image J-based).

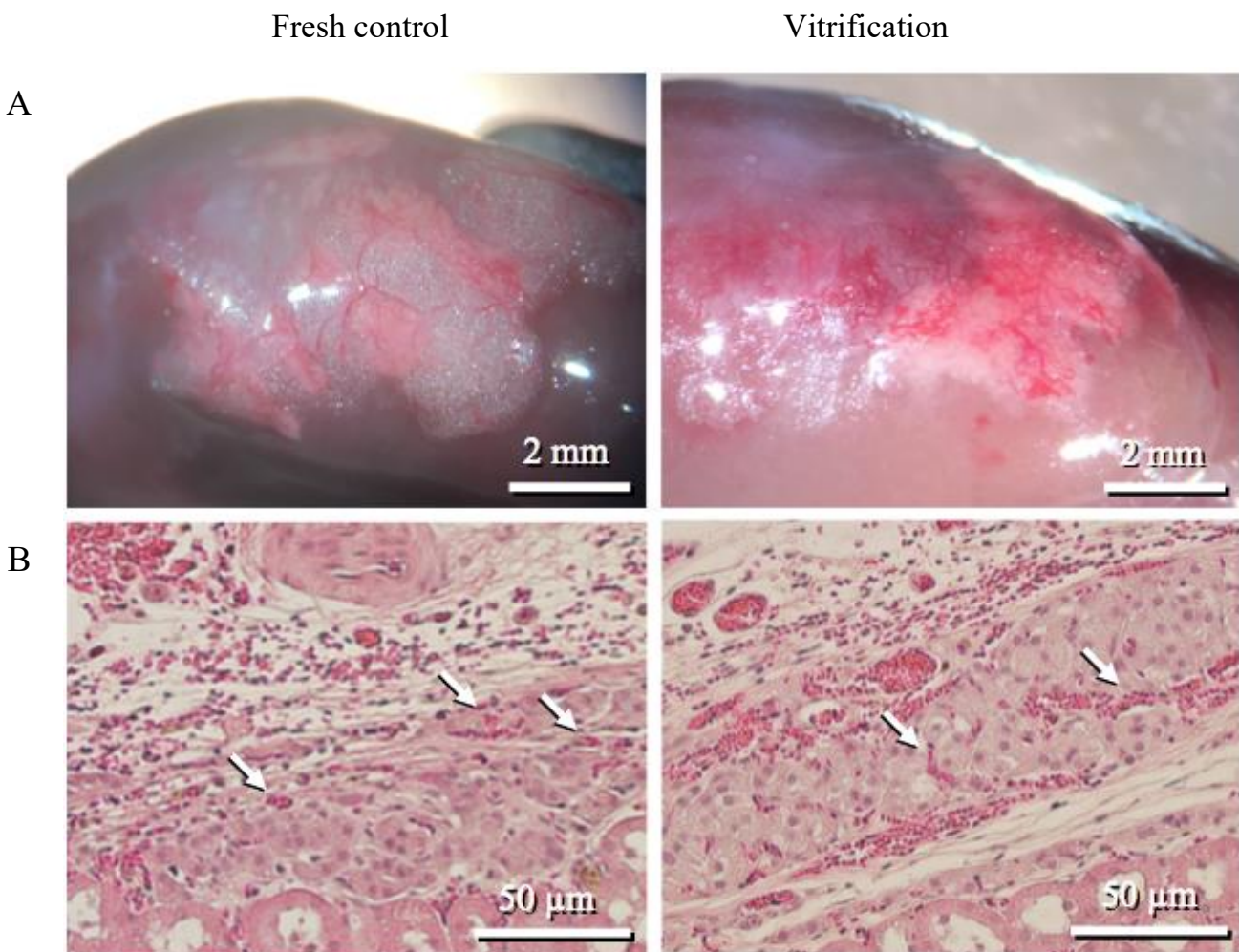


Fig. 4-5. Islet engraft beneath kidney capsule, retrieved from cured recipient rats on Day-70 after transplantation. (A) Islet engrafts (baby pink color), along with angiogenesis. (B) Histological sections of engrafts stained with H&E, showing kidney tissues (bottom part), blood vessels (arrows) and islets.

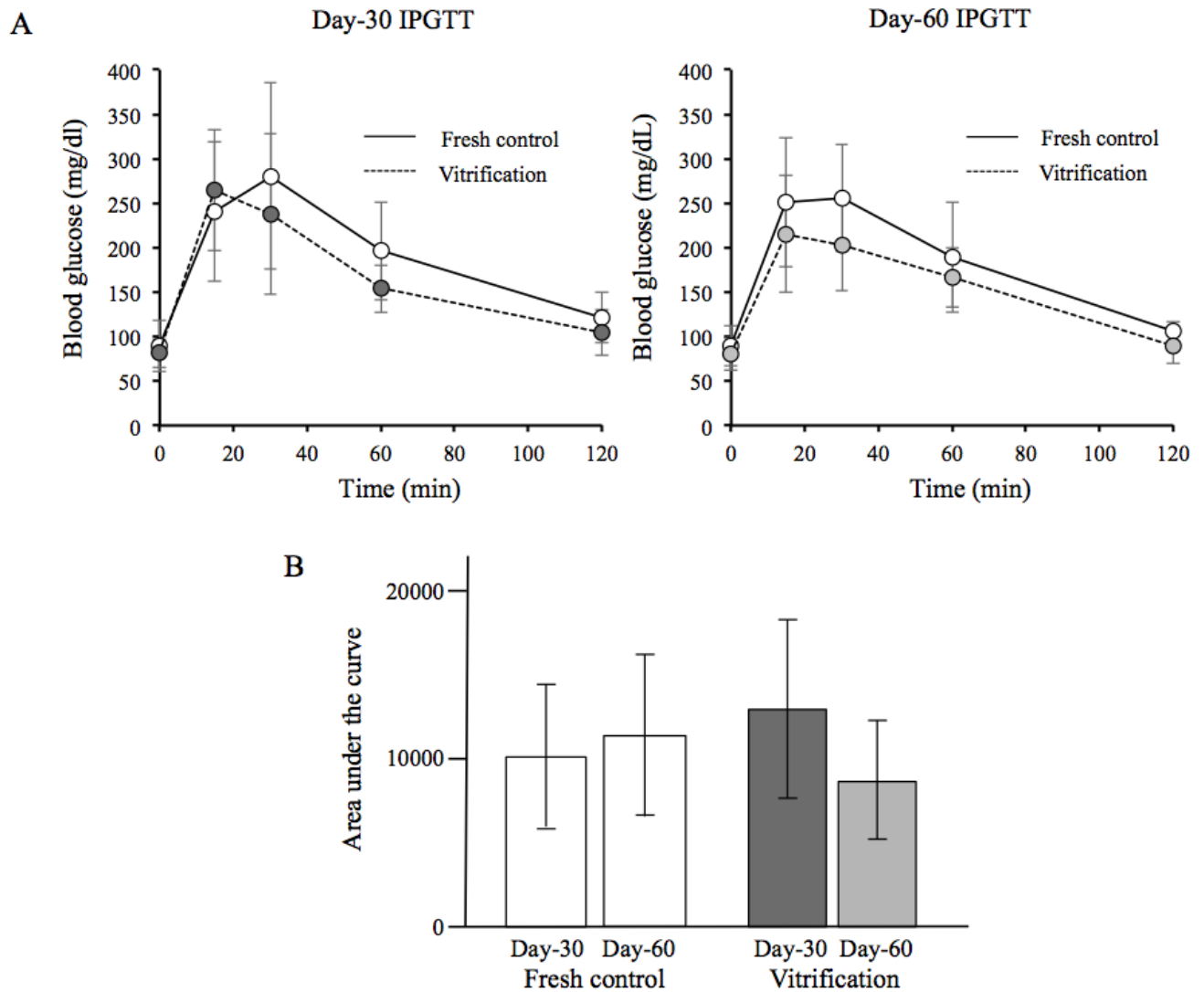


Fig. 4-6. IPGTT (A) and corresponding AUC (B) of cured rats at Day 30 and 60. Mean \pm SEM of 7 and 5 cured recipients in fresh control group and vitrification group, respectively.

IPGTT performed on Day-30 and Day-60 showed similar responses to the glucose uptake of cured rats between fresh control and vitrification groups, including the gradual glycemic control from 15 min to 120 min after glucose administration (**Fig. 4-6 A**). The AUC was also comparable between the fresh control group and the vitrification group, as well as between Day-30 IPGTT and Day-60 IPGTT (**Fig. 4-6 B**).

4.4. Discussion

In the present study, rat islets with the size categories of small (101–150 μm in diameter) plus medium (151–200 μm in diameter) were selected for nylon mesh vitrification and the subsequent subrenal transplantation. Islet number of the mixture can be considered to be the same as the IEQ (islet of a diameter of 150 μm = 1 IEQ) [41]) due to histogram for size-number distribution (data not shown). In addition, the GSIS response was comparable between small size islets and medium size islets (**Table 4-1**). Although the presence of large size islets (17.1%, **Fig. 4-2**) cannot be ignored, their potential of insulin secretion in responses to both 3 and 20 mM glucose stimulation was significantly inferior to that of small size islets (**Table 4-1**). The higher potential of insulin secretion from smaller islets rather than larger islets was reported previously in human [105] as well as rodents (mouse [106] and rat [107]). Several reports [107–110] support the idea that transplants comprised primarily of small rather than large islets may provide preferable graft function, because they are less susceptible to hypoxic damage.

The STZ (glucosamine-nitrosourea compound) is used to prepare hyperglycemia model animals by its particularly toxic effect on insulin-producing β -cells of the pancreas in mammals [112–114]. The STZ is transported through GLUT2 that is highly expressed in the β -cell, and induces cell death by cross-linking with guanine [115, 116]. A high dose of the STZ can induce T1D models, while a low dose of the STZ results in T2D models. In the present syngeneic subrenal transplantation, rat islets vitrified-warmed using nylon mesh devices in a unit of 100 were proven to be functional for glycemic control of the STZ-induced diabetes model rats (**Figs. 4-3, 4-4**). Unstable kinetics of blood glucose level during the first 2 weeks after the syngeneic islet transplantation, occasionally observed both in fresh control and nylon mesh vitrification groups, may be explained by an acute release of insulin stores in β -cells in response to the high blood glucose level of the recipients and the subsequent depletion of the insulin required for maintaining normoglycemia until successful islet engraftment with angiogenesis (**Figs. 4-4, 4-5**). Since 800 islets are often transplanted beneath the kidney capsule of the diabetic recipients in an allogeneic rat model [68, 117], eight repeats per recipient for the preparation of donor islets may be practically acceptable. The larger number of islets has been transplanted to T1D model animals when cryopreserved islets were not equally functional compared to their fresh counterparts [49,

52]. However, such an adjustment in islet number for transplantation was not necessary for our study, probably due to the vitrified-warmed islets carrying enough function for insulin secretion (SI range 4.7; **Table 4-2**). Thus, in vitro assays, including cryosurvival and GSIS, are important tools to determine the utility of cryopreserved islets for transplantation. The islets with an SI value of > 3 in the GSIS are considered suitable for the transplantation [81]. Normal in vivo functionality of the vitrified-warmed islets was further identified with the regained hyperglycemia in recipients after Day-70 nephrectomy (**Fig. 4-4**) and the comparable AUC in IPGTT not only between fresh control and vitrification groups but also between Day-30 and Day-60 (**Fig. 4-6**), suggesting that engrafts of rat islets were responsible for the normoglycemic state.

The islets were vitrified-warmed on the nylon mesh device by minimum volume cooling protocol. Sasamoto *et al.* [49] reported that rat islets vitrified-warmed in VS (EDT324; 30% EG, 20% DMSO and 0.4 M trehalose) by device-free SSV protocol had an SI value of 6.4 and the potential to cure diabetes model recipient rats from hyperglycemia. On the other hand, Nagaya *et al.* [84] reported that functionalities of mouse islets vitrified-warmed in EDT324 by SSV protocol were inferior to those by the HFV protocol, suggesting the rodent species-dependent difference. The most suitable cryopreservation protocol including the VS composition and/or the cryodevice type may also be different between rat islets [83] and hamster islets [73]. Cryoinjury occurs at the periphery of vitrified-warmed islets [83] and β -cells are more likely to be distributed centrally in rodent islets than human islets [118]. Practical use of nylon device without loss of islet recovery, survival and insulin secretion ability (**Table 4-2**) may be further emphasized for suitability of vitrification protocol in efficient islet transplantation. The nylon device does not require the handling of individual islets with glass pipettes, and facilitates the minimization of VS volume surrounding the islets by absorption with a paper towel [111, 119].

In conclusion, the large quantities of rat islets vitrified-warmed on the nylon mesh device were proven fully functional by both in vitro assays (cryosurvival and GSIS) and in vivo assays (subrenal transplantation into diabetes model rats, with IPGTT and histology post-nephrectomy).

4.5. Abstract

Based on some *in vitro* analyses, a large quantity of rat islets could be cryopreserved by vitrification with a nylon mesh device. The aim of the present study was to confirm the adaptability of rat islets vitrified-warmed on the nylon mesh device (100 islets per nylon mesh device) to glycemic control in diabetic model rats. Diabetic BN rats (blood glucose level > 350 mg/dL) were prepared by a single intravenous injection of STZ. Islets with the size categories of small (101–150 μm diameter) and medium (151–200 μm diameter) were selected because the islet number of the mixture was likely the same as the IEQ and GSIS response was comparable between the two categories. The recovery rate of post-warm islets in 101–200 μm diameter from the nylon mesh device was 97.1%. Survival and SI value in GSIS assay were 77.9% and 4.7, respectively (versus fresh control; 97.5% and 6.5, respectively). Post-warm or fresh control islets (800 islets per recipient) were transplanted beneath the kidney capsule of the diabetic rats. Normoglycemia (< 200 mg/dL) was observed at a proportion of 83.3% (5/6) within 3 weeks after the post-warm islet transplantation, comparable with fresh islet transplantation (87.5%; 7/8). IPGTT on Day-30 and Day-60 showed similar 2-h responses to glucose uptake of cured rats between vitrification and fresh control groups. Day-70 nephrectomy confirmed the successful engraftment of transplants through the subsequent diabetes reversal and H&E staining. These results suggest that the large quantities of rat islets vitrified-warmed on nylon mesh devices were proven fully functional both *in vitro* and *in vivo*, due to GSIS and syngeneic transplantation, respectively.

Chapter 5 Conclusive remark

Diabetes mellitus is a group of metabolic diseases characterized by hyperglycemia (fasting blood glucose level, > 125 mg/dL; hemoglobin A1c level, > 6.5%) resulting from defects in insulin secretion and/or insulin action (T2D 90–95% of the cases). Symptoms often include frequent urination, increased thirst, and increased appetite. Diabetes can cause serious long-term complications such as retinopathy, nephropathy, and peripheral neuropathy, if left untreated [1–5]. As of 2019, an estimate of 463 million patients (8.8% of the adult population) had diabetes worldwide, resulting in approximately 4.2 million deaths [6]. The development of inhalable insulin or transdermal insulin in the form of a cream is under clinical investigation. Transplantation of isolated pancreatic islets is a promising treatment alternative to frequent insulin injections, and can restore normoglycemia in patients suffering T1D and, at least in part, T2D [20, 41]. However, a huge number of islets is required for clinical transplantation, because the considerable loss of transplanted islets occurs due to the IBMIR, hypoxia and low nutrient availability until vascularization into engrafts [42–44]. Cryopreservation of pancreatic islets without functional loss can overcome the inevitable shortage of donors and allow time to investigate immunological tissue matching between donors and recipients. Therefore, this study was designed to establish a novel cryopreservation protocol reliable for a higher yield of functional pancreatic islets in the rat diabetes therapy model.

Two cryopreservation protocols (Bicell[®] freezing versus Cryotop[®] vitrification) were compared for their potential to recover the functional rat pancreatic islets. Bicell[®] freezing can provide a constant slow cooling rate ($-0.5^{\circ}\text{C}/\text{min}$) in -80°C deep freezer and widespread for various animal cell types, allowing to treat relatively large quantities of target cells in a freezing vessel. Cryotop[®] vitrification has been developed to accelerate cooling rate ($-23,000^{\circ}\text{C}/\text{min}$) when the devices are plunged into LN₂, and applied mainly for cryopreservation of the larger mammalian embryos and oocytes [64]. Immediate cryosurvival rates of post-thaw and post-warm BN rat islets (101–150 μm diameter), assessed by FDA / PI double staining, were comparable. Most of the PI-positive dead cells were detected in the peripheral area of post-warm

islets, and were removed after subsequent 24 h culture. On the other hand, the dead cells in post-thaw islets distributed not only in their peripheral area but also in the center. Quantitative PCR analysis showed that Bicell[®] freezing compromised expression of genes relating to β -cell function (*Pdx1* and *Glut2*), but not to one of the apoptotic pathways (*Bax* / *Bcl2* ratio). Expression of these genes was maintained in islets before and after the Cryotop[®] vitrification. SI values in GSIS assay, as a parameter of insulin secretion potential, were 6.7, 1.9 and 3.9 in fresh control, post-thaw and post-warm islets, respectively. Larger islets (> 150 μ m diameter) had comparable survival rates, but lower SI values after Cryotop[®] vitrification when compared to smaller counterparts. Thus, rat pancreatic islets can be cryopreserved by Cryotop[®] vitrification rather than Bicell[®] freezing, without considerable loss of in vitro β -cell function [83].

Different cryodevices, such as Cryotop[®] [83], open-pulled straws [68], and hollow fiber [84], have been employed for the vitrification of isolated rodent islets. However, vitrification protocols have a technical limit as large quantities of islets cannot be loaded onto or into each cryodevice (recommended quantity 10–12, possible upper limit 20–30). The limitation depends on necessary treatments, such as CPA equilibration, VS exposure, VS minimization, and CPA dilution, which are difficult to achieve within the required timeframe. Nylon mesh sheet (pore size ϕ = 57- μ m) was the cryodevice originally used to hold as many as 65 bovine immature COCs [65], and was processed as a developed figure of the triangular pyramid for islet vitrification. As the nylon mesh cryodevice does not require the handling of individual islets with glass micropipettes, pre- and post-vitrification islet treatment is less complicated. When a unit of 10 islets was applied to each cryodevice, both the immediate cryosurvival rate of post-warm islets and the SI values in the GSIS assay were comparable between the nylon mesh and the Cryotop[®] vitrification groups. Increased numbers of islets per nylon mesh cryodevice (up to 100) had no adverse effects on the cryosurvival and the insulin secretion potential. Thus, nylon mesh can serve as a simple cryodevice for the vitrification of large quantities of rat pancreatic islets [111].

While the islet insulin secretion potential measured in vitro by the GSIS assay is closely related to the in vivo response for glycemic control of diabetic rodents [49, 68], the adaptability of vitrified-warmed islets to cure hyperglycemia of diabetes model rats needs to be confirmed strictly by islet transplantation. Diabetic BN rats (non-fasting blood glucose level > 350 mg/dL)

were prepared by a single intravenous injection of STZ. Islets with the size categories of small (101–150 μm diameter) and medium (151–200 μm diameter) were selected because the islet number of the mixture was likely the same as the IEQ and GSIS response was comparable between the two categories. One hundred islets were loaded on a nylon mesh cryodevice, and then vitrified-warmed. Diabetic recipient rats received 800 fresh control or vitrified-warmed islets beneath the kidney capsule could achieve normoglycemia (blood glucose level < 200 mg/dL) within 3 weeks after the subrenal islet transplantation, at similar success rates (87.5 and 83.3% in fresh control and nylon mesh vitrification groups, respectively). IPGTT on Day-30 and Day-60 showed similar 2-h responses to the glucose uptake of cured rats between vitrification and fresh control groups. Day-70 nephrectomy confirmed the successful engraftment of transplants through the subsequent diabetes reversal and H&E staining. Thus, the large quantities of rat islets vitrified-warmed on nylon mesh cryodevice were proven fully functional *in vivo* by syngeneic subrenal transplantation [120].

This study, as summarized in **Fig. 5-1**, includes "3S" challenges to establish the novel cryopreservation protocol, which must contain characteristics to deal with practical requirements as "simple operation", "scale-up compatible", and "size variation tolerable". The nylon mesh vitrification [111] seems to be the best promising through both the *in vitro* and *in vivo* assays when compared to the other cryopreservation protocols so far reported [48–53, 56–59, 68, 71–75, 82–84]. As for some beneficial aspects of the "3S" challenges, the simple and easy operation to perform the nylon mesh vitrification enables us to handle the large quantities of small- and medium-sized rat islets. Further technical modifications are necessary until the present findings can contribute directly to the clinical application. However, the progress of the rodent model system would certainly help promote the development of future innovative technology for human diabetes therapy.



Fig. 5-1. Summary of scientific findings in the present study. BN-strain rat islets (101–200 μ m diameter) could be cryopreserved by vitrification using a novel nylon mesh device in a unit of 100 islets. Normal functionality of the post-warm islets was confirmed both in vitro (cryosurvival and GSIS) and in vivo (glycemic control of STZ-induced diabetic BN rats by subrenal transplantation) [83, 111, 120].

References

- [1] N.H. White, W. Sun, P.A. Cleary, R.P. Danis, M.D. Davis, D.P. Hainsworth, L.D. Hubbard, J.M. Lachin, and D.M. Nathan, “Prolonged effect of intensive therapy on the risk of retinopathy complications in patients with type 1 diabetes mellitus: 10 years after the diabetes control and complications trial”, *Arch. Ophthalmol.*, 126, 1707–1715, 2008.
- [2] N. Chaturvedi, M. Porta, R. Klein, T. Orchard, J. Fuller, H.H. Parving, R. Bilous, A.K. Sjølie, and DIRECT Programme Study Group, “Effect of candesartan on prevention (DIRECT-Prevent 1) and progression (DIRECT-Protect 1) of retinopathy in type 1 diabetes: randomised, placebo-controlled trials”, *Lancet*, 372, 1394–1402, 2008.
- [3] P.H. Groop, M.C. Thomas, J.L. Moran, J. Wadèn, L.M. Thorn, V.-P. Mäkinen, M. Rosengård-Bärlund, M. Saraheimo, K. Hietala, O. Heikkilä, C. Forsblom, and FinnDiane Study Group, “The presence and severity of chronic kidney disease predicts all-cause mortality in type 1 diabetes”, *Diabetes*, 58, 1651–1658, 2009.
- [4] M.G. Pezzolesi, G.D. Poznik, J.C. Mychaleckyj, A.D. Paterson, M.T. Barati, J.B. Klein, D.P.K. Ng, G. Placha, L.H. Canani, J. Bochenski, D. Waggott, M.L. Merchant, B. Krolewski, L. Mirea, K. Wanic, P. Katavetin, M. Kure, P. Wolkow, J.S. Dunn, A. Smiles, W.H. Walker, A.P. Boright, S.B. Bull, A. Doria, J.J. Rogus, S.S. Rich, J.H. Warram, A.S. Krolewski, and A.S. Krolewski, “Genome-wide association scan for diabetic nephropathy susceptibility genes in type 1 diabetes”, *Diabetes*, 58, 1403–1410, 2009.
- [5] T.D. Wiggin, K.A. Sullivan, R. Pop-Busui, A. Amato, A.A.F. Sima, and E.L. Feldman, “Elevated triglycerides correlate with progression of diabetic neuropathy”, *Diabetes*, 58, 1634–1640, 2009.
- [6] International Diabetes Federation (IDF Diabetes Atlas Committee, Chair; R. Williams), “IDF Diabetes Atlas 9th edition 2019”, <https://www.diabetesatlas.org/en/>, 2019.
- [7] W. Kerner, J. Brückel, and German Diabetes Association, “Definition, classification and diagnosis of diabetes mellitus”, *Exp. Clin. Endocrinol. Diabetes*, 122, 384–386, 2014.
- [8] D. Dabelea, “The accelerating epidemic of childhood diabetes”, *Lancet*, 373, 1999–2000, 2009.
- [9] G. Imperatore, J.P. Boyle, T.J. Thompson, D. Case, D. Dabelea, R.F. Hamman, J.M. Lawrence, A.D. Liese, L.L. Liu, E.J. Mayer-Davis, B.L. Rodriguez, D. Standiford, and SEARCH for Diabetes in Youth Study Group, “Projections of type 1 and type 2 diabetes burden in the U.S. population aged <20 years through 2050: dynamic modeling of incidence, mortality, and population growth”, *Diabetes Care*, 35, 2515–2520, 2012.

- [10] S. Baekkeskov, J. Kanaani, J.C. Jaume, and S. Kash, “Does GAD have a unique role in triggering IDDM?”, *J. Autoimmun.*, 15, 279–286, 2000.
- [11] J.P. Palmer, C.M. Asplin, P. Clemons, K. Lyen, O. Tatpati, P.K. Raghu, and T.L. Paquette, “Insulin antibodies in insulin-dependent diabetics before insulin treatment”, *Science*, 222, 1337–1339, 1983.
- [12] A. Hattersley, J. Bruining, J. Shield, P. Njolstad, and K.C. Donaghue, “The diagnosis and management of monogenic diabetes in children and adolescents”, *Pediatr. Diabetes*, 10, 33–42, 2009.
- [13] A. Sakula, “Paul Langerhans (1847-1888): a centenary tribute”, *J. R. Soc. Med.*, 81, 414–415, 1988.
- [14] R. Luft, “Oskar Minkowski: discovery of the pancreatic origin of diabetes, 1889”, *Diabetologia*, 32, 399–401, 1989.
- [15] E.L. Opie, “On the histology of the islands of Langerhans of the pancreas”, *Bull. Johns Hopkins Hosp.*, 11, 205–209, 1900.
- [16] M.L. Barr and R.J. Rossiter, “James Bertram Collip, 1892-1965”, *Biogr. Mem. Fellows R. Soc.*, 19, 235–267, 1973.
- [17] L. Hill, "Sir Edward Albert Sharpey-Schafer. 1850-1935", *Biogr. Mem. Fellows R. Soc.*, 1, 400–407, 1935.
- [18] F. Sanger and E.O.P. Thompson, “The amino-acid sequence in the glyceryl chain of insulin. II. The investigation of peptides from enzymic hydrolysates”, *Biochem. J.*, 53, 366–374, 1953.
- [19] T. Blundell, G. Dodson, D. Hodgkin, and D. Mercola, “Insulin: the structure in the crystal and its reflection in chemistry and biology”, *Adv. Protein. Chem.*, 26, 279–402, 1972.
- [20] A.M.J. Shapiro, J.R.T. Lakey, E.A. Ryan, G.S. Korbutt, E. Toth, G.L. Warnock, N.M. Kneteman, and R.V. Rajotte, “Islet transplantation in seven patients with type 1 diabetes mellitus using a glucocorticoid-free immunosuppressive regimen”, *N. Engl. J. Med.*, 343, 230–238, 2000.
- [21] A.R. Saltiel and C.R. Kahn, “Insulin signalling and the regulation of glucose and lipid metabolism”, *Nature*, 414, 799–806, 2001.
- [22] C. Ionescu-Tirgoviste, P.A. Gagniuc, E. Gubceac, L. Mardare, I. Popescu, S. Dima, and M. Militaru, “A 3D map of the islet routes throughout the healthy human pancreas”, *Sci. Rep.*, 5, 14634, 2015.
- [23] Y. Stefan, L. Orci, F. Malaisse-Lagae, A. Perrelet, Y. Patel, and R.H. Unger, “Quantitation of endocrine cell content in the pancreas of nondiabetic and diabetic humans”, *Diabetes*, 31, 694–700, 1982.

- [24] J. Rahier, R.M. Goebbels, and J.C. Henquin, “Cellular composition of the human diabetic pancreas”, *Diabetologia*, 24, 366–371, 1983.
- [25] J. Suckale and M. Solimena, “Pancreas islets in metabolic signaling - focus on the beta cell”, *Front. Biosci.*, 13, 7156–7171, 2008.
- [26] O. Cabrera, D.M. Berman, N.S. Kenyon, C. Ricordi, P.O. Berggren, and A. Caicedo, “The unique cytoarchitecture of human pancreatic islets has implications for islet cell function”, *Proc. Natl. Acad. Sci. U.S.A.*, 103, 2334–2339, 2006.
- [27] L. Orci and R.H. Unger, “Functional subdivision of islets of Langerhans and possible role of D cells”, *Lancet*, 2, 1243–1244, 1975.
- [28] F. Sanger and H. Tuppy, “The amino-acid sequence in the phenylalanyl chain of insulin. 2. The investigation of peptides from enzymic hydrolysates”, *Biochem. J.*, 49, 481–490, 1951.
- [29] M. Liu, M.A. Weiss, A. Arunagiri, J. Yong, N. Rege, J. Sun, L. Haataja, R.J. Kaufman, P. Arvan, “Biosynthesis, structure, and folding of the insulin precursor protein”, *Diabetes Obes. Metab.*, 20 Suppl 2, 28–50, 2018.
- [30] Z. Fu, E.R. Gilbert, and D. Liu, “Regulation of insulin synthesis and secretion and pancreatic Beta-cell dysfunction in diabetes”, *Curr. Diabetes Rev.*, 9, 25–53, 2013.
- [31] M.F. Offield, T.L. Jetton, P.A. Labosky, M. Ray, R.W. Stein, M.A. Magnuson, B.L. Hogan, and C.V Wright, “PDX-1 is required for pancreatic outgrowth and differentiation of the rostral duodenum”, *Development*, 122, 983–995, 1996.
- [32] J.M. Oliver-Krasinski and D.A. Stoffers, “On the origin of the beta cell”, *Genes Dev.*, 22, 1998–2021, 2008.
- [33] G. Waeber, N. Thompson, P. Nicod, and C. Bonny, “Transcriptional activation of the GLUT2 gene by the IPF-1/STF-1/IDX-1 homeobox factor”, *Mol. Endocrinol.*, 10, 1327–1334, 1996.
- [34] Diabetes Control and Complications Trial Research Group, D. M. Nathan, S. Genuth, J. Lachin, P. Cleary, O. Crofford, M. Davis, L. Rand, and C. Siebert, “The effect of intensive treatment of diabetes on the development and progression of long-term complications in insulin-dependent diabetes mellitus”, *N. Engl. J. Med.*, 329, 977–986, 1993.
- [35] A.C. Gruessner, “2011 Update on pancreas transplantation: comprehensive trend analysis of 25,000 cases followed up over the course of twenty-four years at the International Pancreas Transplant Registry (IPTR)”, *Rev. Diabet. Stud.*, 8, 6–16, 2011.
- [36] A.C. Gruessner, D.E.R. Sutherland, and R.W.G. Gruessner, “Long-term outcome after pancreas transplantation”, *Curr. Opin. Organ Transplant.*, 17, 100–105, 2012.

- [37] M.D. Bellin, F.B. Barton, A. Heitman, J.V. Harmon, R. Kandaswamy, A.N. Balamurugan, D.E.R. Sutherland, R. Alejandro, and B.J. Hering, "Potent induction immunotherapy promotes long-term insulin independence after islet transplantation in type 1 diabetes", *Am. J. Transplant.*, 12, 1576–1583, 2012.
- [38] E.A. Ryan, B.W. Paty, P.A. Senior, D. Bigam, E. Alfadhli, N.M. Kneteman, J.R.T. Lakey, and A.M.J. Shapiro, "Five-year follow-up after clinical islet transplantation", *Diabetes*, 54, 2060–2069, 2005.
- [39] A. Gangemi, P. Salehi, B. Hatipoglu, J. Martellotto, B. Barbaro, J.B. Kuechle, M. Qi, Y. Wang, P. Pallan, C. Owens, J. Bui, D. West, B. Kaplan, E. Benedetti, and J. Oberholzer, "Islet transplantation for brittle type 1 diabetes: the UIC protocol", *Am. J. Transplant.*, 8, 1250–1261, 2008.
- [40] A.M.J. Shapiro, J.R.T. Lakey, B.W. Paty, P.A. Senior, D.L. Bigam, and E.A. Ryan, "Strategic opportunities in clinical islet transplantation", *Transplantation*, 79, 1304–1307, 2005.
- [41] E.A. Ryan, J.R. Lakey, R.V. Rajotte, G.S. Korbitt, T. Kin, S. Imes, A. Rabinovitch, J.F. Elliott, D. Bigam, N.M. Kneteman, G.L. Warnock, I. Larsen, and A.M. Shapiro, "Clinical outcomes and insulin secretion after islet transplantation with the Edmonton protocol", *Diabetes*, 50, 710–719, 2001.
- [42] C. Ricordi, D.W. Gray, B.J. Hering, D.B. Kaufman, G.L. Warnock, N.M. Kneteman, S.P. Lake, N.J. London, C. Socci, and R. Alejandro, "Islet isolation assessment in man and large animals", *Acta Diabetol. Lat.*, 27, 185–195, 1990.
- [43] A.M. Davalli, Y. Ogawa, C. Ricordi, D.W. Scharp, S. Bonner-Weir, and G.C. Weir, "A selective decrease in the beta cell mass of human islets transplanted into diabetic nude mice", *Transplantation*, 59, 817–820, 1995.
- [44] W. Bennet, B. Sundberg, C.G. Groth, M.D. Brendel, D. Brandhorst, H. Brandhorst, R.G. Bretzel, G. Elgue, R. Larsson, B. Nilsson, and O. Korsgren, "Incompatibility between human blood and isolated islets of Langerhans: a finding with implications for clinical intraportal islet transplantation?", *Diabetes*, 48, 1907–1914, 1999.
- [45] E. Cantarelli and L. Piemonti, "Alternative transplantation sites for pancreatic islet grafts", *Curr. Diab. Rep.*, 11, 364–374, 2011.
- [46] A. Rajab, "Islet transplantation: alternative sites", *Curr. Diab. Rep.*, 10, 332–337, 2010.
- [47] S. Marani, C. Toso, J. Emamaullee, and A.M. Shapiro, "Optimal implantation site for pancreatic islet transplantation", *Br. J. Surg.*, 95, 1449–1461, 2008.

- [48] G.L. Warnock, N.M. Kneteman, E. Ryan, R.E. Seelis, A. Rabinovitch, and R.V. Rajotte, “Normoglycemia after transplantation of freshly isolated and cryopreserved pancreatic islets in type 1 (insulin-dependent) diabetes mellitus”, *Diabetologia*, 34, 55–58, 1991.
- [49] H. Corominola, J. Mendola, E. Esmatjes, A. Sáenz, L. Fernández-Cruz, and R. Gomis, “Cryopreservation of pancreatic islets prior to transplantation: a comparison between UW solution and RPMI culture medium”, *Cryobiology*, 37, 110–118, 1998.
- [50] F. Liu, W. Tian, Y. Yang, Q. Zhang, M. Zhu, L. Yang, L. Yang, J. Li, J. Liu, P. Wu, K. Yang, X. Wang, Y. Shen, and Z. Qi, “Optimal method for short-term or long-term islet preservation: comparison of islet culture, cold preservation and cryopreservation”, *J. Artif. Organs*, 17, 337–343, 2014.
- [51] N.M. Kneteman, D. Alderson, D.W. Scharp, and P.E. Lacy, “Long-term cryogenic storage of purified adult human islets of Langerhans”, *Diabetes*, 38, 386–396, 1989.
- [52] J. Mendola, H. Corominola, J.M. Gonzalez-Clemente, E. Esmatjes, A. Saenz, L. Fernandez-Cruz, and R. Gomis, “Follow-up study of the revascularization process of cryopreserved islets of Langerhans”, *Cryobiology*, 33, 530–543, 1996.
- [53] R.V. Rajotte, M.G. Evans, G.L. Warnock, and N.M. Kneteman, “Islet cryopreservation”, *Horm. Metab. Res.*, 25, 72–81, 1990.
- [54] G.M. Fahy, D.R. MacFarlane, C.A. Angell, and H.T. Meryman, “Vitrification as an approach to cryopreservation”, *Cryobiology*, 21, 407–426, 1984.
- [55] W.F. Rall and G.M. Fahy, “Ice-free cryopreservation of mouse embryos at –196 degrees C by vitrification”, *Nature*, 313, 573–575, 1985
- [56] N.H.P.M. Jutte, P. Heyse, H.G. Jansen, G.J. Bruining, and G.H. Zeilmaker, “Vitrification of mouse islets of Langerhans: comparison with a more conventional freezing method”, *Cryobiology*, 24, 292–302, 1987.
- [57] N.H. Jutte, P. Heyse, H.G. Jansen, G.J. Bruining, and G.H. Zeilmaker, “Vitrification of human islets of Langerhans”, *Cryobiology*, 24, 403–411, 1987.
- [58] S. Langer, D. Lau, T. Eckhardt, H. Jahr, H. Brandhorst, D. Brandhorst, B.J. Hering, K. Federlin, and R.G. Bretzel, “Viability and recovery of frozen-thawed human islets and in vivo quality control by xenotransplantation”, *J. Mol. Med.*, 77, 172–174, 1999.
- [59] M.J. Taylor and S. Baicu, “Review of vitreous islet cryopreservation: Some practical issues and their resolution”, *Organogenesis*, 5, 155–166, 2009.
- [60] Practice Committees of American Society for Reproductive Medicine and Society for Assisted Reproductive Technology, “Mature oocyte cryopreservation: a guideline”, *Fertil. Steril.*, 99, 37–43, 2013.

- [61] A. Martino, N. Songsasen, and S.P. Leibo, “Development into blastocysts of bovine oocytes cryopreserved by ultra-rapid cooling”, *Biol. Reprod.*, 54, 1059–1069, 1996.
- [62] G. Vajta, P. Holm, M. Kuwayama, P.J. Booth, H. Jacobsen, T. Greve, and H. Callesen, “Open Pulled Straw (OPS) vitrification: a new way to reduce cryoinjuries of bovine ova and embryos”, *Mol. Reprod. Dev.*, 51, 53–58, 1998.
- [63] M. Lane, W.B. Schoolcraft, and D.K. Gardner, “Vitrification of mouse and human blastocysts using a novel cryoloop container-less technique”, *Fertil. Steril.*, 72, 1073–1078, 1999.
- [64] M. Kuwayama, G. Vajta, O. Kato, and S.P. Leibo, “Highly efficient vitrification method for cryopreservation of human oocytes”, *Reprod. Biomed. Online*, 11, 300–308, 2005.
- [65] H. Matsumoto, J.Y. Jiang, T. Tanaka, H. Sasada, and E. Sato, “Vitrification of large quantities of immature bovine oocytes using nylon mesh”, *Cryobiology*, 42, 139–144, 2001.
- [66] Y. Abe, K. Hara, H. Matsumoto, J. Kobayashi, H. Sasada, H. Ekwall, H. Rodriguez-Martinez, and E. Sato, “Feasibility of a nylon-mesh holder for vitrification of bovine germinal vesicle oocytes in subsequent production of viable blastocysts”, *Biol. Reprod.*, 72, 1416–1420, 2005.
- [67] I-S. Hwang, H. Hara, H.-J. Chung, M. Hirabayashi, and S. Hochi, “Rescue of vitrified-warmed bovine oocytes with Rho-associated coiled-coil kinase inhibitor”, *Biol. Reprod.*, 89, 26, 2013.
- [68] H. Sasamoto, M. Futami, Y. Ando, and S. Nakaji, “Cryopreservation of rat islets of Langerhans by vitrification”, *J. Artif. Organs*, 15, 283–289, 2012.
- [69] M. Hirabayashi and S. Hochi, “Rat embryonic stem cells: establishment and their use for transgenesis”, In: *Methodological Advances in the Culture, Manipulation and Utilization of Embryonic Stem Cells for Basic and Practical Applications* (Ed. C. Atwood), InTech, 397–410, 2011.
- [70] S. Hochi, T. Terao, M. Kamei, M. Kato, M. Hirabayashi, and M. Hirao, “Successful vitrification of pronuclear-stage rabbit zygotes by minimum volume cooling procedure”, *Theriogenology*, 61, 267–275, 2004.
- [71] M.J. Taylor and S. Baicu, “Review of vitreous islet cryopreservation: some practical issues and their resolution”, *Organogenesis*, 5, 155–166, 2009.
- [72] G.L. Warnock, J.R. Lakey, Z. Ao, and R.V. Rajotte, “Tissue banking of cryopreserved islets for clinical islet transplantation”, *Transplant. Proc.*, 26, 3438, 1994.
- [73] C.A. Agudelo and H. Iwata, “The development of alternative vitrification solutions for microencapsulated islets”, *Biomaterials*, 29, 1167–1176, 2008.

- [74] S. Matsumoto, M. Matsushita, T. Morita, H. Kamachi, S. Tsukiyama, Y. Furukawa, S. Koshida, Y. Tachibana, S.-I. Nishimura, and S. Todo, “Effects of synthetic antifreeze glycoprotein analogue on islet cell survival and function during cryopreservation”, *Cryobiology*, 52, 90–98, 2006.
- [75] I. Sakonju, Y. Taura, K. Mamba, T. Suzuki, K. Takimoto, M. Nakaichi, and S. Nakama, “Differential freezing tolerance of rat pancreatic islets depending on their size variation”, *J. Vet. Med. Sci.*, 57, 859–863, 1995.
- [76] J.-C. Martinou and D.R. Green, “Breaking the mitochondrial barrier”, *Nat. Rev. Mol. Cell Biol.*, 2, 63–67, 2001.
- [77] C.K. Colton, K.K. Papas, A. Pisania, M.J. Rappel, D.E. Powers, J.J. O’Neil, A. Omer, G. Weir, and S. Bonner-Weir, “Characterization of islet preparations”, In: *Cellular Transplantation* (Eds. C. Halberstadt and D. Emerich), Academic Press, 85–133, 2007.
- [78] M.J. Barnett, D. McGhee-Wilson, A.M.J. Shapiro, and J.R.T. Lakey, “Variation in human islet viability based on different membrane integrity stains”, *Cell Transplant.*, 13, 481–488, 2004.
- [79] F. Bertuzzi and C. Ricordi, “Prediction of clinical outcome in islet allotransplantation”, *Diabetes Care*, 30, 410–417, 2007.
- [80] K.K. Papas, T.M. Suszynski, and C.K. Colton, “Islet assessment for transplantation”, *Curr. Opin. Organ Transplant.*, 14, 674–682, 2009.
- [81] N. Sakata, S. Egawa, S. Sumi, and M. Unno, “Optimization of glucose level to determine the stimulation index of isolated rat islets”, *Pancreas*, 36, 417–423, 2008.
- [82] M.A. von Mach, J. Schlosser, M. Weiland, P.J. Feilen, M. Ringel, J.G. Hengstler, L.S. Weilemann, J. Beyer, P. Kann, and S. Schneider, “Size of pancreatic islets of Langerhans: a key parameter for viability after cryopreservation”, *Acta Diabetol.*, 40, 123–129, 2003.
- [83] T. Yamanaka, K. Tashima, R. Takahashi, S. Takashima, T. Goto, M. Hirabayashi, and S. Hochi, “Direct comparison of Cryotop[®] vitrification and Bicell[®] freezing on recovery of functional rat pancreatic islets”, *Cryobiology*, 73, 376–382, 2016.
- [84] M. Nagaya, H. Matsunari, T. Kanai, M. Maehara, K. Nakano, I. Umeki, Y. Katsumata, Y. Kasai, R. Sakai, M. Kobayashi, M. Honda, N. Abe, M. Watanabe, K. Umeyama, and H. Nagashima, “An effective new cryopreservation procedure for pancreatic islets using hollow fiber vitrification”, *Horm. Metab. Res.*, 48, 540–549, 2016.
- [85] S. Chinen, T. Yamanaka, K. Nakayama, H. Watanabe, Y. Akiyama, M. Hirabayashi, and S. Hochi, "Nylon mesh cryodevice for bovine mature oocytes, easily removable excess vitrification solution", *Cryobiology*, 90, 96–99, 2019.

- [86] S. Chinen, T. Yamanaka, M. Hirabayashi, and S. Hochi, "Rescue of vitrified-warmed bovine mature oocytes by short-term recovery culture with resveratrol", *Cryobiology*, 97, 185–190, 2020.
- [87] A. Dinnyés, Y. Dai, S. Jiang, and X. Yang, "High developmental rates of vitrified bovine oocytes following parthenogenetic activation, in vitro fertilization, and somatic cell nuclear transfer", *Biol. Reprod.*, 63, 513–518, 2000.
- [88] H. Matsunari, M. Maehara, K. Nakano, Y. Ikezawa, Y. Hagiwara, N. Sasayama, A. Shirasu, H. Ohta, M. Takahashi, and H. Nagashima, "Hollow fiber vitrification: a novel method for vitrifying multiple embryos in a single device", *J. Reprod. Dev.*, 58, 599–608, 2012.
- [89] M. Maehara, H. Matsunari, K. Honda, K. Nakano, Y. Takeuchi, T. Kanai, T. Matsuda, Y. Matsumura, Y. Hagiwara, N. Sasayama, A. Shirasu, M. Takahashi, M. Watanabe, K. Umeyama, Y. Hanazono, and H. Nagashima, "Hollow fiber vitrification provides a novel method for cryopreserving in vitro maturation/fertilization-derived porcine embryos", *Biol. Reprod.*, 87, 133, 2012.
- [90] A. Uchikura, H. Matsunari, K. Nakano, S. Hatae, and H. Nagashima, "Application of hollow fiber vitrification for cryopreservation of bovine early cleavage stage embryos and porcine morula-blastomeres", *J. Reprod. Dev.*, 62, 219–223, 2016.
- [91] J.H. Juang, C.H. Kuo, and B.R. Hsu, "Effects of multiple site implantation on islet transplantation", *Transplant. Proc.*, 34, 2698–2699, 2002.
- [92] D. Yin, J.W. Ding, J. Shen, L. Ma, M. Hara, and A.S. Chong, "Liver ischemia contributes to early islet failure following intraportal transplantation: benefits of liver ischemic-preconditioning", *Am. J. Transplant.*, 6, 60–68, 2006.
- [93] A.R. Pepper, R. Pawlick, A. Bruni, B. Gala-Lopez, J. Wink, Y. Rafiei, M. Bral, N. Abualhassan, and A.M. Shapiro, "Harnessing the foreign body reaction in marginal mass device-less subcutaneous islet transplantation in mice", *Transplantation*, 100, 1474–1479, 2016.
- [94] Y. Yasunami, Y. Nakafusa, N. Nitta, M. Nakamura, M. Goto, J. Ono, and M. Taniguchi, "A novel subcutaneous site of islet transplantation superior to the liver", *Transplantation*, 102, 945–953, 2018.
- [95] K-M. Lee, J-H. Kim, E-S. Choi, E. Kim, S-K. Choi, and W.B. Jeon, "RGD-containing elastin-like polypeptide improves islet transplantation outcomes in diabetic mice", *Acta Biomater.*, 94, 351–360, 2019.
- [96] F. Li, Y. Lv, X. Li, Z. Yang, T. Guo, and J. Zhang, "Comparative study of two different islet transplantation sites in mice: Hepatic sinus tract vs splenic parenchyma", *Cell. Transplant.*, 29, 96389720943576, 2020.

- [97] J.I. Stagner, H.L. Rilo, and K.K. White, "The pancreas as an islet transplantation site. confirmation in a syngeneic rodent and canine autotransplant model", *J. Pancreas*, 8, 628–636, 2007.
- [98] M. Morikawa, T. Kimura, M. Murakami, K. Katayama, S. Terada, and A. Yamaguchi, "Rat islet culture in serum-free medium containing silk protein sericin", *J. Hepatobiliary Pancreat Surg.*, 16, 223–228, 2009.
- [99] E. Estil les, N. Téllez, J. Escoriza, and E. Montanya, "Increased β -cell replication and β -cell mass regeneration in syngeneically transplanted rat islets overexpressing insulin-like growth factor II", *Cell Transplant.*, 21, 2119–2129, 2012.
- [100] Y. He, M. Zhang, Y. Wu, H. Jiang, H. Fu, Y. Cai, Z. Xu, C. Liu, B. Chen, and T. Yang, "Aberrant activation of Notch-1 signaling inhibits podocyte restoration after islet transplantation in a rat model of diabetic nephropathy", *Cell Death Dis.*, 9, 950, 2018.
- [101] X. Zhu, F. Guo, H. Tang, C. Huang, G. Xie, T. Huang, Y. Li, C. Liu, H. Wang, and B. Chen, "Islet transplantation attenuating testicular injury in type 1 diabetic rats is associated with suppression of oxidative stress and inflammation via Nrf-2/HO-1 and NF- κ B pathways", *J. Diabetes Res.*, 2019, 8712492, 2019.
- [102] A.A. Hardikar, M.V. Risbud, C. Remacle, B. Reusensm J.J. Hoet, and R.R. Bhone, "Islet cryopreservation: Improved recovery following taurine pretreatment", *Cell Transplant.*, 10, 247–253, 2001.
- [103] H-H. Huang, L. Novikova, S.J. Williams, I.V. Smirnova, and L. Stehno-Bittel, "Low insulin content of large islet population is present in situ and in isolated islets", *Islets*, 3, 6–13, 2011.
- [104] B. Farhat, A. Almelkar, K. Ramachandran, S.J. Williams, H-H. Huang, D. Zamierowski, L. Novikova, and L. Stehno-Bittel, "Small human islets comprised of more β -cells with higher insulin content than large islets", *Islets*, 5, 87–94, 2013.
- [105] Y. Fujita, M. Takita, M. Shimada, T. Itoh, K. Sugimoto, H. Noguchi, B. Naziruddin, M.F. Levy, and S. Matsumoto, "Large human islets secrete less insulin per islet equivalent than smaller islets in vitro", *Islets*, 3, 1–5, 2011.
- [106] K-H. Nam, W. Yong, T. Harvat, A. Adewola, S. Wang, J. Oberholzer, and D.T. Eddington, "Size-based separation and collection of mouse pancreatic islets for functional analysis", *Biomed Microdevices*, 12, 865–874, 2010.
- [107] R.R. MacGregor, S.J. Williams, P.Y. Tong, K. Kover, W.V. Moore, and L. Stehno-Bittel, "Small rat islets are superior to large islets in in vitro function and in transplantation outcomes", *Am. J. Physiol. Endocrinol. Metab.*, 290, E771–E779, 2006.

- [108] D. Zorzi, T. Phan, M. Sequi, Y. Lin, D.H. Freeman, L. Cicalese, and C. Rastellini, "Impact of islet size on pancreatic islet transplantation and potential interventions to improve outcome", *Cell Transplant.*, 24, 11–23, 2015.
- [109] Z. Su, J. Xia, W. Shao, Y. Cui, S. Tai, H. Ekberg, M. Corbascio, J. Chen, and Z. Qi, "Small islets are essential for successful intraportal transplantation in a diabetes mouse model", *Scand. J. Immunol.*, 72, 504–510, 2010.
- [110] R. Lehmann, R.A. Zuellig, P. Kugelmeier, P.B. Baenninger, W. Moritz, A. Perren, P-A. Clavien, M. Weber, and G.A. Spinas, "Superiority of small islets in human islet transplantation", *Diabetes*, 56, 594–603, 2007.
- [111] T. Yamanaka, T. Goto, M. Hirabayashi, and S. Hochi, "Nylon mesh device for vitrification of large quantities of rat pancreatic islets", *Biopreserv Biobank*, 15, 457–462, 2017.
- [112] K.R. Mansford and L. Opie, "Comparison of metabolic abnormalities in diabetes mellitus induced by streptozotocin or by alloxan", *Lancet*, 1, 670–671, 1968.
- [113] C.C. Rerup, "Drugs producing diabetes through damage of the insulin secreting cells", *Pharmacol. Rev.*, 22, 485–518, 1970.
- [114] I.M. Murray-Lyon, A.L. Eddleston, R. Williams, M. Brown, B.M. Hogbin, A. Bennett, J.C. Edwards, and K.W. Taylor, "Treatment of multiple-hormone-producing malignant islet-cell tumour with streptozotocin", *Lancet*, 2, 895–898, 1968.
- [115] Z. Wang and H. Gleichmann, "GLUT2 in pancreatic islets: crucial target molecule in diabetes induced with multiple low doses of streptozotocin in mice", *Diabetes*, 47, 50–56, 1998.
- [116] W.J. Schnedl, S. Ferber, J.H. Johnson, and C.B. Newgard, "STZ transport and cytotoxicity. Specific enhancement in GLUT2-expressing cells", *Diabetes*, 43, 1326–1333, 1994.
- [117] K. Ohnishi, M. Murakami, M. Morikawa, and A. Yamaguchi, "Effect of the silk protein sericin on cryopreserved rat islets", *J. Hepatobiliary Pancreat Sci.*, 19, 354–360, 2012.
- [118] J. Dolensek, M.S. Rupnik, and A. Stozer, "Structural similarities and differences between the human and the mouse pancreas", *Islets*, 7, e1024405, 2015.
- [119] K. Nakayama, T. Yamanaka, Y. Tamada, M. Hirabayashi, and S. Hochi, "Supplementary cryoprotective effect of carboxylated ϵ -poly-L-lysine during vitrification of rat pancreatic islets", *Cryobiology*, 88, 70–74, 2019.
- [120] K. Nakayama-Iwatsuki, T. Yamanaka, J. Negishi, J. Teshima, Y. Tamada, M. Hirabayashi, and S. Hochi, "Transplantation of rat pancreatic islets vitrified-warmed on the nylon mesh device and the silk fibroin sponge disc", *Islets*, 12, 145–155, 2020.

List of publications

Original articles, directly related to doctoral dissertation

- [1] **T. Yamanaka**, K. Tashima, R. Takahashi, S. Takashima, T. Goto, M. Hirabayashi, and S. Hochi, “Direct comparison of Cryotop[®] vitrification and Bicell[®] freezing on recovery of functional rat pancreatic islets”, *Cryobiology*, 73, 376–382, 2016.
- [2] **T. Yamanaka**, T. Goto, M. Hirabayashi, and S. Hochi, “Nylon mesh device for vitrification of large quantities of rat pancreatic islets”, *Biopreserv Biobank*, 15, 457–462, 2017.
- [3] K. Nakayama-Iwatsuki, **T. Yamanaka**, J. Negishi, J. Teshima, Y. Tamada, M. Hirabayashi, and S. Hochi, "Transplantation of rat pancreatic islets vitrified-warmed on the nylon mesh device and the silk fibroin sponge disc", *Islets*, 12, 145–155, 2020.

Reference original articles

- [1] M. Hirabayashi, H. Hara, T. Goto, A. Takizawa, M.R. Dwinell, **T. Yamanaka**, S. Hochi, and H. Nakauchi, “Haploid embryonic stem cell lines derived from androgenetic and parthenogenetic rat blastocysts”, *J. Reprod. Dev.*, 63, 611–616, 2017.
- [2] K. Masaki, M. Sakai, S. Kuroki, J. Jo, K. Hoshina, Y. Fujimori, K. Oka, T. Amano, **T. Yamanaka**, M. Tachibana, Y. Tabata, T. Shinozawa, O. Ishizuka, S. Hochi, and S. Takashima, “Spermatogonial self-renewal factor FGF2 has distinct functions from GDNF in the mouse germline niche”, *Stem Cell Rep.*, 10, 1782–1792, 2018.
- [3] K. Nakayama, **T. Yamanaka**, Y. Tamada, M. Hirabayashi, and S. Hochi, "Supplementary cryoprotective effect of carboxylated ϵ -poly-L-lysine during vitrification of rat pancreatic islets", *Cryobiology*, 88, 70–74, 2019.
- [4] S. Chinen, **T. Yamanaka**, K. Nakayama, H. Watanabe, Y. Akiyama, M. Hirabayashi, and S. Hochi, "Nylon mesh cryodevice for bovine mature oocytes, easily removable excess vitrification solution", *Cryobiology*, 90, 96–99, 2019.
- [5] S. Chinen, **T. Yamanaka**, M. Hirabayashi, and S. Hochi, "Rescue of vitrified-warmed bovine mature oocytes by short-term recovery culture with resveratrol", *Cryobiology*, 97, 185–190, 2020.

Acknowledgments

First of all, I would like to express my sincere gratitude to my supervisor, Professor Dr. Shinichi HOCHI (Faculty of Textile Science and Technology, Shinshu University, Ueda, Nagano, Japan) for all of his helpful guidance in the preparation of this thesis and support throughout the study. I wish to express my special appreciation to Associate Professor Dr. Masumi HIRABAYASHI (Center for Genetic Analysis of Behavior, National Institute for Physiological Sciences, Okazaki, Aichi, Japan), Dr. Teppei GOTO (RIKEN Center for Biosystems Dynamics Research, Kobe, Hyogo, Japan), Associate Professor Dr. Seiji TAKASHIMA, and Research Associate Dr. Jun NEGISHI (Faculty of Textile Science and Technology, Shinshu University, Ueda, Nagano, Japan) for their help throughout the study. Professor Dr. Keisuke EDASHIGE (Faculty of Agriculture and Marine Sciences, Kochi University, Nankoku, Kochi, Japan), Professor Dr. Yasushi TAMADA, Professor Dr. Tomoaki HORIE, and Associate Professor Dr. Yoshitake AKIYAMA (Faculty of Textile Science and Technology, Shinshu University, Nagano, Japan) are acknowledged for their effort and valuable advice to review and improve this thesis. I want to express my thankful mind to all of HOCHI's lab student members for their co-working and cooperation in research, and finally to my parents for their continuous encouragement and warm supports.

Funding

My challenge for the Ph.D. degree was supported by the Doctor-21 program of Yoshida Scholarship Foundation (2018–2020) and by a research grant of Nagano Society for the Promotion of Science (2019).



Universal blue circle symbol for diabetes. World Diabetes Day was launched in 1991 by the International Diabetes Federation (IDF) and the World Health Organization (WHO) in response to the rapid increase of diabetes around the world. The day is held on 14 November each year, which marks the birthday of Frederick BANTING who first discovered insulin in 1921.